J. Fluid Mech. (1986), *vol.* 173, *pp.* 387–429
Printed in Great Britain

Quantum turbulence

By RUSSELL J. DONNELLY AND CHARLES E. SWANSON
Department of Physics, University of Oregon, Eugene, OR 97403, USA

(Received 14 March 1986)

We present a review of quantum turbulence, that is, the turbulent motion of quantized vortex lines in superfluid helium. Our discussion concentrates on the turbulence produced by steady, uniform heat flow in a pipe, but touches on other turbulent flows as well. We have attempted to motivate the study of quantum turbulence and discuss briefly its connection with classical turbulence. We include background on the two-fluid model and mutual friction theory, examples of modern experimental techniques, and a brief survey of the phenomenology. We discuss the important recent insights that vortex dynamics has provided to the understanding of quantum turbulence, from simple scaling arguments to detailed numerical simulations. We conclude with a discussion of open questions in this field.

1. Introduction

This symposium is properly dedicated to many subjects in classical fluid dynamics which will demonstrate, we are certain, that the spirit of G. I. Taylor is very much active in our research community, It is, therefore, with some trepidation that we present a discussion of a topic where the investigation has developed quite separately from those lines of research associated with Taylor's name and work, and which has really only recently been recognized as an independent field of inquiry. Our subject is the turbulent motion of quantized vortex lines in superfluid helium. We are aware that many of our collegues in fluid mechanics regard the study of superfluidity as a remote, arcane and technically formidable discipline. We would note that the temperatures ranges we are concerned with were experimentally accessible in G. I. Taylor's younger years, that the frontier in low temperature physics is at temperatures more than three orders of magnitude lower than those dealt with in this paper, and that the basic techniques are no more demanding than many modern fluid mechanics investigators encounter in their daily work.

We would like to demonstrate that, once the details of the production and maintenance of low temperatures are accepted as routine, the leading intellectual approaches to our subject have been very much in the spirit of G. I. Taylor: simple experiments based upon a profound knowledge of the underlying questions to be addressed.

Our group has been active in research in this field for some years. We present an overview of our own experimental work and ideas, together with the work of other groups which constitute our view of what is important in the subject. Our account is, therefore, not a balanced review of the subject, which we believe has been burdened with experiments which have accumulated mountains of data with little overall purpose. We are fortunate that Tough (1982) has undertaken a survey of this vast accumulation of data and has succeeded in identifying certain key characteristics. In particular he has proposed a classification of four turbulent states which allows

considerable insight into the database. The existence of this, and other modern reviews, allows us to cite the reviews as secondary sources with considerable economy of space. For authoritative information, the primary sources should always be consulted.

The plan of this paper is as follows. Section 2 on early history and ideas contains historical material and a general discussion of the phenomenon of quantum turbulence. Our motivation in studying the phenomenon and certain related questions are discussed in §3, while §4 describes some important and representative modern experimental methods. Section 5 contains a survey of current knowledge of turbulence produced by steady counterflow. Section 6 contains a brief discussion of vortex dynamics and the information one can obtain by scaling arguments, while §7 reviews the insights and current limitations of numerical simulations of vortex dynamics. Section 8 contains a description of turbulence generated by other flows, i.e. flows with divergent heat flux, non-zero mass flux, or unsteady heat flux, a subject currently less well developed than that due to steady counterflow, but interesting nonetheless. Section 9 contains a summary discussion, and enumeration of some important and basic unsolved problems.

2. Early history and ideas

2.1. *Leiden measurements*

The early history of our subject begins with investigations at Leiden University on the thermal conductivity of liquid helium. Under its own vapour pressure, helium remains a liquid from its normal boiling point at 4.2 K to absolute zero. Liquid helium in the temperature range from 4.2 K to the lambda transition at $T_\lambda = 2.172$ K is called helium I and that from T_λ down to absolute zero, helium II. Helium I boils and has classical fluid properties. Helium II is absolutely quiescent and exhibits superfluidity. Helium I and helium II exist under pressure as well. The early history of the discovery of the lambda transition is outlined in a recent publication by Donnelly & Francis (1985).

Keesom & Keesom (1936) measured the thermal conductivity of helium I in the apparatus of figure 1 (*a*). The liquid was contained in a cylindrical layer L of diameter 3.6 cm and depth 0.5 cm. The top and bottom of the cell consisted of copper blocks A and B, each containing a heater and thermometer. At $T = 3.3$ K the authors obtained a thermal conductivity of 6×10^{-5} cal/deg cm^{-1} s^{-1}, which is of the order of magnitude of the conductivity of gasses at ordinary temperatures. The thermal conductivity of helium II, on the other hand, is so great that a capillary tube must be used to observe a temperature gradient, The first systematic measurements were by Keesom, Keesom & Saris (1938) using the apparatus of figure 1 (*b*). A, B, C and D are copper pieces containing chambers a, b, c and d filled with liquid helium through metal capillaries. Capillaries of different width and length were used between B and C. B and C also contained thermometers and a heater was attached to A. The authors found that the heat conductivity has a pronounced maximum at 1.7 to 2.0 K with conductivities as high as 810 cal/deg cm^{-1} s^{-1}, i.e. more than 800 times that of copper at room temperature, and 1.3×10^7 the value obtained for helium I. Keesom & Keesom called helium II 'supra-heat conducting', with good justification.

It is interesting that the devices illustrated in figure 1 are in use today in more or less the same form. The helium I cell appears today in the *Journal of Fluid Mechanics* as a Bénard convection cell (cf. Pfotenhauer, Lucas & Donnelly 1984). The so-called 'counterflow' apparatus of figure 1 (*b*) still represents one of the most

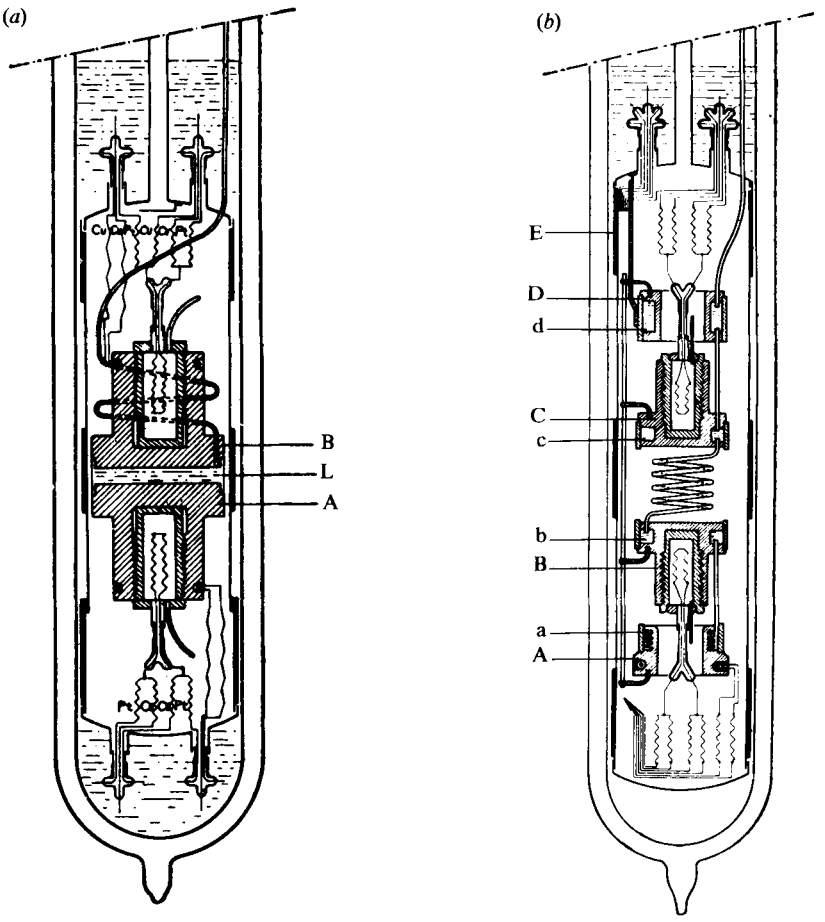

FIGURE 1. Apparatus for determining: (*a*) the thermal conductivity of helium I (Keesom & Keesom 1936), (*b*) the relationship between heat flux and temperature gradient in helium II (Keesom, Keesom & Saris 1938). The components are discussed in the text.

important and fundamental techniques for studying the flow of helium II: a heat source, and thermometers to measure the temperature gradient. A modern vision of this apparatus is discussed in §4.1. One can also construct chemical potential probes in place of thermometers, as we shall discuss in §4.4 below.

2.2. *Superfluidity*

The ability of helium II to flow through narrow channels without dissipation was discovered simultaneously by Kapitza (1938) and Allen & Misener (1938) and named 'superfluidity' by Kapitza, by analogy to the frictionless flow of electrons in a superconductor.

It is interesting that the main thread of our story begins with the work of P. L. Kapitza, who was in Cambridge in the 1930s, and was a colleague of G. I. Taylor. We shall perhaps never know what conversations Kapitza and Taylor had on low temperature phenomena, but G. I. Taylor did tell one of us (R.J.D.) that he had significant conversations with Kapitza about the design of the helium gas bearing support of the piston used in the low temperature expansion engine of a Kapitza

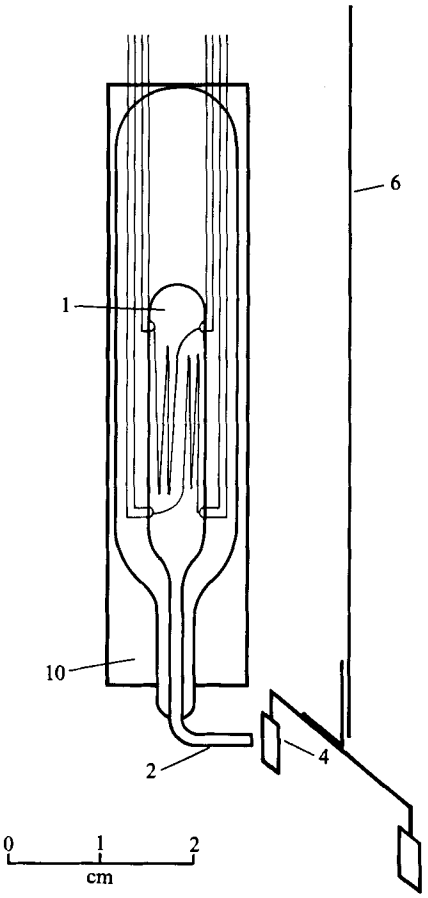

FIGURE 2. Kapitza's apparatus designed to study the jet of normal fluid emerging from a counterflow apparatus. The superfluid is supposed to enter the channel in potential flow and therefore does not disturb the vane (Kapitza 1941).

liquifier. This same principle is used in most modern helium liquifiers in operation in the world today.

2.3. *Kapitza's early experiments*

The exigencies of politics (Badash 1985) took Kapitza from Cambridge to Moscow, where he began an investigation of the extraordinarily high heat transport through narrow channels filled with helium II and the small viscosity associated with this flow state. Kapitza (1941) built a number of different experimental arrangements: in one of them a counterflow capillary was equipped with a rotating inner rod so that the effect of stirring could be studied (it reduced the thermal conductivity). This is the first instance of the study of the flow of helium II between concentric cylinders. This subject is recently reconsidered in a paper by Donnelly & LaMar (1986). In figure 2 a torsionally suspended vane, 4, was used to measure the force of the normal fluid jet emerging from the counterflow apparatus, 1, containing a heater and thermometer through capillary 2. The chief contribution of these experiments was to establish some of the spectacular properties of helium II and set the stage for the theoretical work of Landau.

The thermohydrodynamics of helium II has been studied extensively since the work described above. Discussions of the dramatic properties of helium II are contained in many sources: for hydrodynamically oriented readers an article by Roberts & Donnelly (1974) contains much of the theory and experiment relevant to our present purposes. We shall give a few paragraphs here to orient the reader and to establish notation.

2.4. *The two-fluid model and second sound*

Helium II acts hydrodynamically as if it were a mixture of a normal fluid of density ρ_n, velocity $\boldsymbol{v}_n$ and a superfluid, of density ρ_s and velocity $\boldsymbol{v}_s$. The superfluid appears to carry no entropy, and the entire heat content of the fluid must be added to convert a mass of superfluid to normal fluid. The total density,

$$\rho = \rho_n + \rho_s, \tag{2.1}$$

is about 0.14 g/cm^3. Under modest chemical potential gradients the superfluid can flow with no measurable friction, and flow states can be set up in toroidal geometries which appear to persist indefinitely.

The normal fluid has a viscosity of order 20 μp and tends to be immobilized in porous powders of size less than about 1 μm. The superfluid, however, is not so hindered, and flows easily through the finest channels one can manufacture. Porous media, then, form a semipermeable separator for helium II, passing the superfluid and not normal fluid. A temperature difference ΔT across such a barrier, will develop a 'fountain pressure' ΔP, and these variables are related to the entropy per unit mass S, by

$$\frac{\Delta P}{\Delta T} = \rho S. \tag{2.2}$$

Suppose liquid helium is contained in a tube with a closed end fitted with a heater, as shown schematically in figure 3, and the heater supplies heat flux q (Watts/cm^2). When heat is supplied, the superfluid will flow towards the heater, pick up heat content, transform to normal fluid and flow away from the heater out to the helium bath. This peculiar counterflow has no net mass flux, i.e.

$$\boldsymbol{j} = \rho_n \boldsymbol{v}_n + \rho_s \boldsymbol{v}_s = 0, \tag{2.3}$$

and since the superfluid has no entropy, the heat flux is $q = \rho S T \boldsymbol{v}_n$. If the heat is switched on and off periodically, the two fluids will execute small amplitude counterflow described by a standing wave of second sound. Second sound is a wave of temperature difference in helium II which has low natural attenuation and very little dispersion. Second sound is an important tool in quantum turbulence research because second sound is attenuated by quantized vortices.

The combined evidence of the above and other experiments leads to the two-fluid equations of motion (for a rigorous discussion, see Roberts & Donnelly 1974)

$$\rho_s \frac{\mathrm{D}\boldsymbol{v}_s}{\mathrm{D}t} = -\frac{\rho_s}{\rho}\nabla P + \rho_s S \nabla T - \boldsymbol{F}_{ns}, \tag{2.4}$$

$$\rho_n \frac{\mathrm{D}\boldsymbol{v}_n}{\mathrm{D}t} = -\frac{\rho_n}{\rho}\nabla P - \rho_s S \nabla T + \boldsymbol{F}_{ns} + \eta \nabla^2 \boldsymbol{v}_n \tag{2.5}$$

where η is the coefficient of shear viscosity and $\boldsymbol{F}_{ns}$ is a mutual friction force between the normal fluid and superfluid which we will discuss in §2.6 below, and which is zero

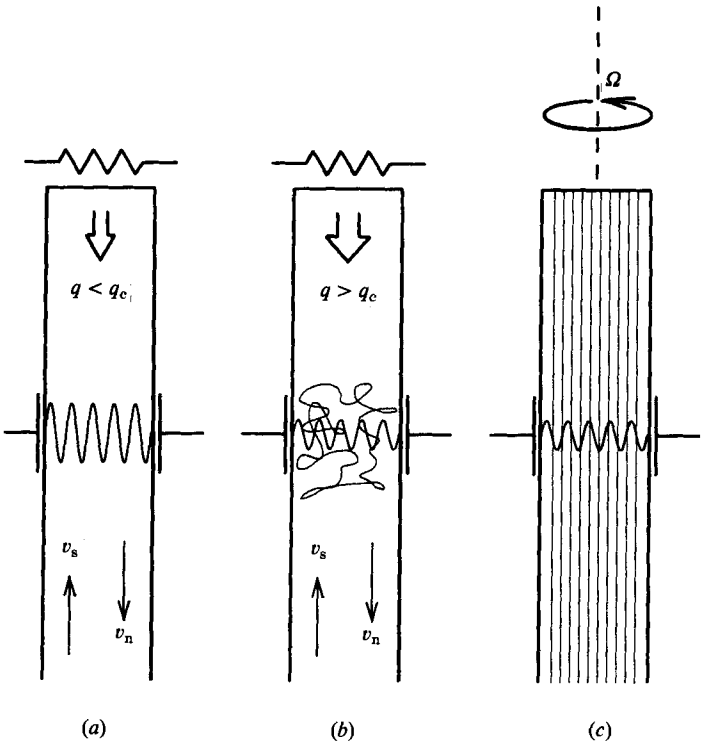

FIGURE 3. Schematic diagram of a thermal counterflow apparatus for studying quantum turbulence. Second sound transducers are represented on the side walls with a resonance excited between them. (*a*) $q < q_c$ (*b*) $q > q_c$ (*c*) rotation only.

in the absence of vortex lines. To these are added conservation equations for mass and entropy

$$\frac{\partial \rho}{\partial t} + \operatorname{div}(\rho_s \boldsymbol{v}_s + \rho_n \boldsymbol{v}_n) = 0, \tag{2.6}$$

$$\frac{\partial}{\partial t}\rho s + \operatorname{div}(\rho S \boldsymbol{v}_n) = 0, \tag{2.7}$$

and the equation for the flow of the superfluid

$$\operatorname{curl} \boldsymbol{v}_s = 0. \tag{2.8}$$

These equations lead to, among other things, equations for the propagation of first and second sound.

2.5. *Quantized vortices and rotation*

Equation (2.8) was at first thought to deny rotation to the superfluid fraction of helium II altogether, but Osborne (1950) found that the rotation of helium II was indistinguishable from that of helium I. Following the suggestion of the quantization of circulation by Onsager (1949) and the theory of vortex lines in rotating helium by Feynman (1955), Hall & Vinen (1956*a*, *b*) verified Feynman's prediction that in a bucket of rotating helium II, the normal fluid rotates uniformly with the bucket but the superfluid vorticity $\boldsymbol{\omega} = \operatorname{curl} \boldsymbol{v}_s$ appears as a uniform array of discrete vortex lines parallel to the axis of rotation (see figure 3*c*). For most purposes, a quantized

vortex line can be thought of as a classical vortex line in the superfluid with a hollow core of radius a (about one ångstrom) and quantized circulation

$$\oint \boldsymbol{v}_s \cdot d\boldsymbol{l} = \frac{h}{m} = \kappa, \tag{2.9}$$

where the integration encircles the core, h is Planck's constant and m the mass of the helium atom: $\kappa \approx 9.97 \times 10^{-4}$ cm^2 s^{-1}. In a bucket rotating at angular velocity Ω radians per second the areal density of vortex lines, n_v, is the same as the line density L measured as length of line per unit volume (cm/cm^3 = cm^{-2}), and is given by the ratio of the vorticity of solid body rotation to the quantum of circulation:

$$n_v \doteq L = \frac{2\Omega}{\kappa} \approx 2000\,\Omega \text{ lines cm}^{-2}. \tag{2.10}$$

Vortex lines appear in more general flows as well, such as the flow between rotating cylinders and in the counterflow experiment described above. In the latter the vortex lines appear only after some critical heat flux q_c, and seem to be nearly randomly oriented with respect to the flow as suggested in figure 3(*b*). The vortices are sometimes described as a 'tangled mass', and densities up to the order of 10^5 cm^{-2} are easily generated. A review of the structure and dynamics of quantized vortex lines has recently appeared (Glaberson & Donnelly 1986).

2.6. *Mutual friction in helium II*

Gorter & Mellink (1949), motivated by experiments on pressure and temperature differences down to narrow channels, proposed that the extra dissipation above that owing to viscosity alone could be adequately represented by the addition of a mutual friction term to the equations of motion. This term is now usually written as

$$\boldsymbol{F}_{ns} = -\rho_s \rho_n A v_{ns}^2 \boldsymbol{v}_{ns}, \tag{2.11}$$

where $\boldsymbol{v}_{ns} = \boldsymbol{v}_n - \boldsymbol{v}_s$, $v_{ns} = |\langle \boldsymbol{v}_{ns} \rangle|$, and A is a function of T (and in principle v_{ns}) and is of order 50 cm s^{-1} g^{-1}. The broken brackets denote spatial and temporal averages. This form of $\boldsymbol{F}_{ns}$ is useful for vortex turbulence work in channels, and is most frequently used in the steady state with time averaged quantities.

Studies by Hall & Vinen (1956*a*,*b*) showed that a second sound wave propagating across uniformly rotating helium II (see figure 3*c*) is attenuated by the vortices, whereas propagation axially, i.e. parallel to $\boldsymbol{\Omega}$, produces no attenuation. They deduced that the mutual friction term in (2.4) and (2.5) for rotating helium II should be

$$\boldsymbol{F}_{ns} = \frac{B\rho_s\rho_n}{\rho\Omega}\boldsymbol{\Omega} \times (\boldsymbol{\Omega} \times \boldsymbol{v}_{ns}) + \frac{B'\rho_s\rho_n}{\rho}\boldsymbol{\Omega} \times \boldsymbol{v}_{ns}, \tag{2.12}$$

where B and B' are mutual friction parameters depending on temperature, second sound frequency, and flow velocity. The mutual friction force (2.12) gives rise to an extra contribution α_L to the attenuation of second sound:

$$\alpha_L = \frac{B\Omega}{2u_2} = \frac{B\kappa L}{4u_2}, \tag{2.13}$$

the latter relationship to line density in rotation coming from (2.10). For a current, detailed discussion of mutual friction, see Barenghi, Donnelly & Vinen (1983) and Swanson *et al.* (1986).

Much of the study of quantum turbulence is done in steady state pipe flow. The

time and cross-sectional averages of (2.4) and (2.5) in steady state (the 'mutual friction approximation') are, to first order,

$$0 = -(\rho_S/\rho)\langle \nabla T\rangle - \langle \boldsymbol{F}_{ns}\rangle, \tag{2.14}$$

$$0 = -(\rho_N/\rho)\langle \nabla P\rangle - \rho_s S\langle \nabla T\rangle + \langle \boldsymbol{F}_{ns}\rangle + \eta\langle \nabla^2 \boldsymbol{v}_n\rangle, \tag{2.15}$$

where brackets denote time and cross-sectional averages. Adding (2.14) and (2.15), we find

$$\langle \nabla P\rangle = \eta\langle \nabla^2 \boldsymbol{v}_n\rangle, \tag{2.16}$$

which suggests that the pressure gradient ∇P in turbulent superflow is not much different to that in laminar (Poiseuille) flow. This is known to be roughly true, and is called 'the Allen and Reekie rule'. A second-order term that is ignored here is $-\langle \rho_n(\boldsymbol{v}_n \cdot \nabla)\boldsymbol{v}_n\rangle$, a term we feel is important for its qualitative effects, although it is not of much importance quantitatively for analysing experiments. We will say more about this in §9.

With a laminar mean flow assumption, we have for the pressure gradient

$$\nabla P_L = -\frac{G\eta \boldsymbol{v}_n}{d^2}, \tag{2.17}$$

where G is a factor known theoretically for Poiseuille flow for each channel shape and d is the channel size. The thermodynamic potential gradient per unit mass, usually called the chemical potential in the helium II literature, vanishes in laminar flow:

$$\nabla \mu_L = -S\nabla R_L + \frac{\nabla P_L}{\rho} = 0, \tag{2.18}$$

consistent with dissipationless flow for the superfluid. Thus the laminar flow temperature gradient is

$$\nabla T_L = \frac{\nabla P_L}{\rho S} = -\frac{G\eta \boldsymbol{v}_n}{\rho S d^2}. \tag{2.19}$$

In turbulent flow, the total temperature gradient is

$$\nabla T = \nabla T_L + \nabla T_T, \tag{2.20}$$

where ∇T_T is, neglecting the increase in ∇P above the laminar value,

$$\nabla T_T = \frac{\boldsymbol{F}_{ns}}{S\rho_s}, \tag{2.21}$$

and since F_{ns} varies roughly as v_{ns}^3, the neglect of the extra pressure gradient becomes quantitatively reasonable for large flow rates. The chemical potential gradient is given by

$$\nabla \mu = -\frac{\boldsymbol{F}_{ns}}{\rho_s}. \tag{2.22}$$

This shows that dissipation owing to vortices produces a direct change in chemical potential. We shall describe a detector for this quantity in §4.4.

The connection of the mutual friction coefficients to line length per unit volume may be seen by a simple analogy. In uniform rotation, from (2.10) and (2.12), the dissipative term of $\boldsymbol{F}_{ns}$ parallel to $\boldsymbol{v}_{ns}$ has the magnitude $B\rho_s\rho_n\kappa L/2\rho$. For turbulent flow the assumption is that mutual friction acts in the same manner on each segment of vortex line in a tangle as it does on an array produced by rotation; but that in second sound attenuation, for example, an average of one-third of the vortex line segments in the tangle will be oriented parallel to the second sound propagation

direction and not detected. Thus for isotropically oriented vortex lines, the magnitude of the dissipative part of the mutual friction term can be written

$$F_{ns} = -\frac{B\rho_s\rho_n\kappa}{2\rho}\tfrac{2}{3}L_0 v_{ns}, \tag{2.23}$$

where $L_0 = \langle L \rangle$. For a more careful discussion of the relationship between second sound measurements and the properties of the tangle, see Swanson (1985) or Swanson & Donnelly (1985).

The boundary conditions for the two-fluid model are straightforward. Generally one assumes that neither normal nor superfluid components can flow into a boundary, that the normal component has zero tangential velocity at a wall, and the superfluid can slip. Ordinarily one would believe that the temperature T would be continuous between a solid and liquid helium, but the Kapitza resistance phenomenon (see, for example, Pfotenhauer & Donnelly 1985) shows that T is not continuous in the presence of a heat flux into a boundary. The appropriate boundary conditions in the presence of moving vortices are not well understood (see Glaberson & Donnelly 1986 for a discussion of what is known) and may be important in understanding the normal fluid velocity profile above critical (see §9).

2.7. *Vinen's theory*

A model for the development of the tangle of quantized vortex lines, developed from the ideas of mutual friction, was introduced by Vinen in a classic series of papers (Vinen 1957*a–c*, 1958). This theory considers a spatially homogeneous distribution of vortex lines whose time rate of change is determined by competing growth and decay processes. Vinen derived the growth term by dimensional analysis and modelled the decay process after the decay of classical turbulence in the Kolmogorov cascade. He obtained

$$\frac{dL}{dt} = \chi_1 B\rho_n v_{ns} L^{\frac{3}{2}} - \frac{\chi_2\kappa L^2}{2\pi}, \tag{2.24}$$

where χ_1 and χ_2 are undetermined parameters. In steady state $\langle dL/dt \rangle = 0$ and the equilibrium line density is

$$L_0 = \gamma^2 v_{ns}^2, \tag{2.25}$$

where $\gamma = \pi B\rho_n\chi_1/\kappa\rho\chi_2$. The v_{ns}^2 dependence of L_0 predicted by Vinen's model is roughly correct above the critical heat flux (see §5.1). γ, which contains the temperature dependence, has to be determined experimentally since χ_1 and χ_2 are not known.

3. Motivation and goals for the study of quantum turbulence

3.1. *Is quantum turbulence really turbulence?*

The readers of the *Journal of Fluid Mechanics* are well aquainted with the enormous complexities of turbulent flow in classical fluid mechanics. There is certainly challenge enough in that subject to occupy anyone's attention. Why then should effort be put into the study of quantum turbulence?

To begin, one might ask whether quantum turbulence is turbulence? Let us consider several well-known features of classical turbulence and compare them to quantum turbulence. We follow here a development of ideas by Tennekes & Lumley (1972).

(i) *Irregularity.* Experimental evidence is that quantized vortex lines in turbulent flow are random. Counterflow channels show homogeneous, but not isotropic,

distribution of vortex line density. The power spectral density of fluctuations is flat from 0 to about 1 Hz, then falls off in a fashion resembling a low pass electrical filter circuit. Simulations of self-sustaining vortex structures in helium II produce irregular configurations.

(ii) *Diffusivity.* Classical turbulent flows are highly diffusive, leading to much higher intensities of transport processes than one finds from uncorrelated molecular motion (kinetic theory). It has been stated that quantum turbulence is not diffusive, and evidence for this is the sharp decrease in line density away from a region of high counterflow velocities (see §8.3). We feel that this is evidence for a lack of diffusion *away* from the turbulent region, but there is evidence for a great increase in transport processes within the turbulent region. The normal fluid velocity profile is essentially flat in turbulent counterflow (see §5.5), so that it is not at all like Poiseuille flow, suggesting a great increase in momentum transport.

(iii) *Large Reynolds numbers.* Classical turbulence often originates as an instability of laminar flows if the Reynolds number becomes too large. Flows in helium II exhibit similar instabilities as the normal and superfluid velocities rise. Since the viscosity of the superfluid is strictly zero, the Reynolds numbers involved are, in some sense, infinite.

(iv) *Three-dimensional vorticity fluctuations.* Tennekes & Lumley (1972) say 'vorticity dynamics plays an essential role in the description of turbulent flows'. It often seems that in quantum turbulence it plays the *only* role of importance, though there is some evidence to the contrary (see §9). We shall see that what is measured in experiments in helium II is the magnitude of the vorticity, and motion of this vorticity is required for the dissipation observed (Anderson 1966). There is evidence from vortex simulations that the three-dimensional nature of the motion is crucial for a self-sustaining tangle (Schwarz 1985).

(v) *Dissipation.* The superfluid is inviscid and cannot by itself dissipate energy. But quantized vortex lines couple the normal and superfluid components by mutual friction and can lead to large levels of energy dissipation, much greater than the viscosity of the normal fluid alone could produce.

(vi) *Continuum.* Quantum turbulence is described as a continuum phenomenon (see, for example, §2.7). The vortices are generally spaced by quite macroscopic distances (> 1 μm), and when distances between vortex cores decrease to the order of the core size, quantum mechanics enters the problem. Quantum mechanics is, of course, also a continuum theory. A very nice connection between quantum mechanics and hydrodynamics is given by the Madelung transformation (see, for example, Jones & Roberts 1982).

(vii) *Turbulence is not a unique feature of a given fluid.* Classical turbulence is not a property of a fluid, but of a flow. One might at first think that quantum turbulence is unique to the superfluid, and this would certainly be true at absolute zero. But experiments are done in helium II which is all superfluid at absolute zero and all normal fluid at the lambda transition. The ratios ρ_n/ρ and ρ_s/ρ vary over orders of magnitude. Applying pressure makes enormous changes in the properties of helium II. Adding ^{3}He to the ^{4}He also produces profound differences. Indeed a whole class of 'tailored' superfluids can be made by making mixtures of ^{3}He and ^{4}He and applying pressure. The turbulence properties of these fluids have not yet been studied in detail. Pure ^{3}He itself becomes superfluid at about 1 mK, and has quantized vortices as well. The properties of turbulence in superfluid ^{3}He have not yet been addressed.

There are also differences between the study of classical and quantum turbulence.

In classical turbulence, vortex stretching is very important for two reasons: it increases the vorticity in a volume and it decreases the lengthscale of the eddies (Tennekes & Lumley 1972). The lengthscale decrease leads to an energy cascade, eventually allowing the eddies to be efficiently killed by viscosity. In quantum turbulence the picture is similar to a point: vortex stretching still leads to longer lines and to crowding of the lines (see Baym & Chandler 1983). A difference arises because of the lack of superfluid viscosity, so the lengthscale decrease due to crowding does not kill the lines in the classical manner. Instead, mutual friction and boundary interactions lead to most of the vortex line decrease. Another difference arises because classical vortex stretching shrinks the core (concentrates the vorticity), whereas quantum vortex stretching cannot change the core of an individual vortex line (its structure being fixed with the temperature). The process will be the same only in the continuum limit. Townsend (1961) has argued that a continuum representation is probably only useful for isothermal flow, i.e. where there is no counterflow.

A major experimental difference is that much of the classical work involves measurements of local velocities and their correlations, whereas in quantum turbulence no local probe has yet been developed and measurements reflect a volume averaged vorticity. Further conceptual differences come from the nearly singular vorticity distribution, the 'slip' boundary condition for the superfluid velocity, the additional degrees of freedom resulting from the (partial) uncoupling of convective mass and heat transport, and the dependence of the normal and superfluid densities on v_{ns}^2 (cf. Roberts & Donnelly 1974 §*d*).

3.2. *Is quantum turbulence really quantum mechanics?*

By and large, phenomena in the hydrodynamics of helium II obey classical hydrodynamics, often beyond the range where one might confidently use continuum models. For example, the mean atomic spacing in liquid helium is about 3.6 Å, but the best current estimate for the vortex core size (Glaberson & Donnelly 1986) is about 0.8 Å, or one quarter of the interatomic spacing. This suprisingly small core radius can occur because the velocity of the superfluid is considered to be given by the gradient of the phase of the order parameter (for a discussion of these terms see, for example, Vinen 1966) and the order parameter is the square of the amplitude of a nonlinear Schrödinger equation. In such a continuum description the interatomic spacing does not arise directly, although it must obviously set the order of magnitude of the smallest scales. Let us give an example of a phenomenon which overlaps classical and quantum descriptions.

Rotons, the most prevalent excitations of the superfluid, have a wavelength $\lambda \approx 3.3$ Å, comparable to the interatomic spacing. Rotons are known to have a strong fluid dipole moment of strength $\mu = P/4\pi\rho$, where $P = \hbar q$, which gives rise to strong interactions between them. These interactions take the form of scattering and binding of rotons. Scattering (unbound) orbits in a classical theory (Roberts & Donnelly 1973, 1974) have an average critical impact parameter of about 6.7 Å, in good agreement with experiments determining the roton viscosity. The binding energy is known experimentally to be (-0.22 ± 0.07) K (Murray, Woerner & Greytak 1975). This quantity was calculated classically by Roberts & Donnelly (1973, 1974) and they obtained a value of about -18.4 K with a stable separation of about 1.05 Å. The result conflicts violently with experiment. A quantum mechanical treatment of the binding of two rotons (Roberts & Pardee 1974) amends the mean separation to about 12 Å, and the binding energy to about -0.29 K, in substantial agreement with experiment. We see that the interaction of two rotons at a distance substantially

closer than their associated deBroglie wavelength is a quantum mechanical problem, and we expect that the interaction of a vortex line and a roton or of two vortex lines at similar distances to also be a quantum mechanical problem.

The fate of two elements of vortex line which approach closely is called the 'reconnection' problem. It involves quantum mechanics. We shall return to a discussion of reconnection in §7.3 below.

The circulation about a vortex line is strictly quantized in the unit $\kappa = h/m$. We can safely conclude that quantum mechanics is an important part of quantum turbulence. Indeed, if $h \to 0$, the problem would not exist.

3.3. *Why should we bother to study quantum turbulence?*

Classical turbulence has more than enough interest and challenge to occupy any investigator's attention. If one were to try to justify putting time and effort into studying quantum turbulence one might advance the following arguments:

(i) The turbulence of fluids in general remains one of the major unsolved problems in physics.

(ii) Quantum turbulence is easy to produce, compact in scale, and in a fluid of basically simple and accurately known properties.

(iii) Quantum turbulence is manifest over an enormous range of physical variables. Channel sizes (the 'wind tunnels' for quantum turbulence) span four orders of magnitude: from micrometres to centimetres. The superfluid fraction ρ_s/ρ varies from unity at low temperatures to 10^{-2} and even 10^{-3} as experiments are conducted near T_λ. We believe that experiments near the lambda transition are in a very interesting regime for study. Vortex densities L can easily vary over five orders of magnitude.

(iv) In counterflow experiments, at least, the normal fluid is probably in laminar, or weakly turbulent flow; hence the effect of its motion is not likely to be a major conceptual barrier to the understanding of the total flow.

(v) The laws of vortex dynamics appear to be fairly well understood on a fundamental level, as discussed in §6.

(vi) The laws which govern the ability of a vortex tangle to be sustained in a flow should be able to be understood quantitatively on the basis of vortex dynamics. The decay of a vortex tangle to heat (i.e. rotons and phonons) is a major challenge which may be easier to understand than the corresponding problem in classical turbulence, because the vorticity is confined to one-dimensional lines with quantized circulation.

(vii) The heat transfer in counterflow has practical applications in cooling superconducting devices (Pfotenhauer & Donnelly 1985).

The list of what we would like to know about quantum turbulence is very large. Some of the important questions might include the following:

(i) How are quantized vortices nucleated? Do pre-existing vortices play a crucial role?

(ii) How do quantized vortex structures grow and decay and extract energy from the flow? How do quantized vortices reconnect on contact?

(iii) How do vortex structures decay into heat?

(iv) What is the nature of vortex structures: their configuration, motion, interactions and statistical properties?

4. Modern experimental methods

The most common studies of quantum turbulence are temperature-difference measurements in narrow channels and second sound attenuation measurements in wide channels. We shall describe two modern experimental set-ups as examples of

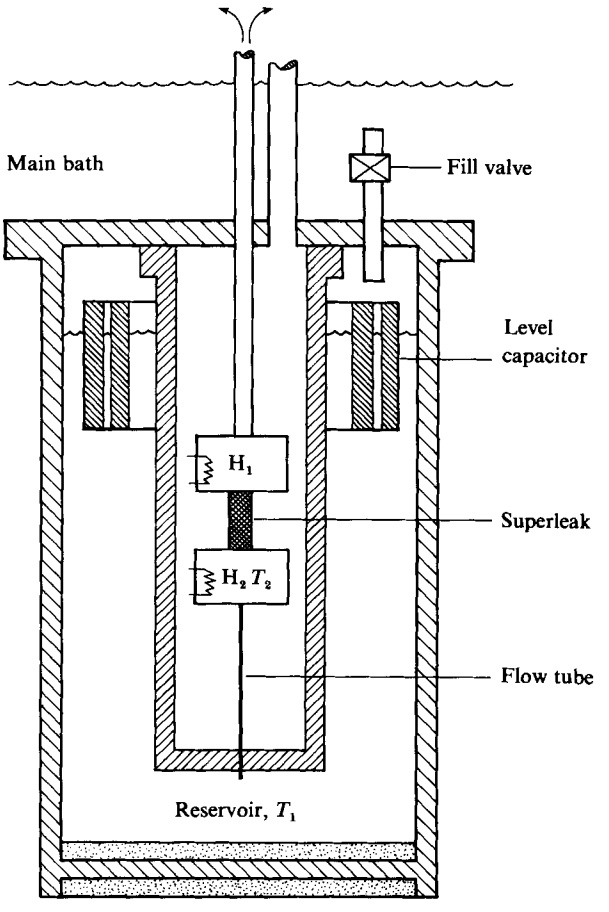

FIGURE 4. Apparatus designed by Baehr & Tough (1985). The operation is described in the text.

current techniques, as well as a novel device to measure chemical potential differences. Examples of ion measurements and generation of shock waves conclude this section. These are representative of current techniques, and other apparatus will be described in the appropriate sections.

4.1. *Temperature-difference measurements in narrow channels*

We have already described the standard capillary tube experiment of Keesom *et al.* (1938). A modern apparatus reported by Baehr & Tough (1985) has the advantage that flows of arbitrary v_n and v_s can be generated at will.

The apparatus is shown in figure 4. The flow tube ('wind tunnel') is about 0.01 cm inside diameter and connected between a large reservoir at temperature T_1 and a small reservoir at temperature T_2 containing a heater H_2. A further small reservoir containing a heater H_1 is connected by a superleak, allowing superfluid flow, but not normal flow, nor (of course) heat flow.

Applying electric current to H_1 pumps superfluid from the reservoir at T_1 to the main helium bath. The superfluid flux through the experimental flow tube, and thus the (average) superfluid velocity v_s, is determined by the liquid level capacitor (the level decrease as liquid flows out decreases the capacitance, since helium gas has a lower dielectric constant than the liquid). Normal fluid flow is produced in the flow

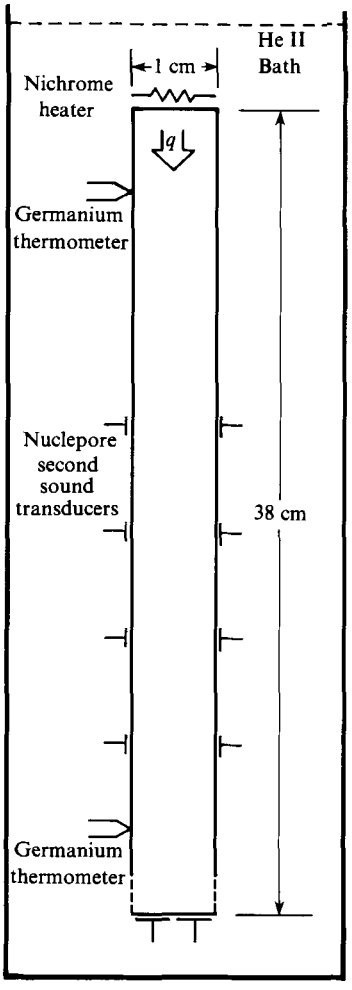

FIGURE 5. Schematic of one possible arrangement of wide channel interchangeable sections used at the University of Oregon. Both transverse and axial second sound transducers are shown.

capillary tube by energizing heater H_2. Since no heat can pass through the superleak, the average normal fluid velocity v_n is given by $q/\rho ST$.

The experiment can be run in a pure counterflow mode by leaving the fountain pump H_1 off. For $q < q_c$ the only dissipation is due to the normal fluid viscosity, and the temperature difference ΔT is given by (2.19). Equation (2.19) is sufficiently accurate that it can be used to determine the average diameter d of the flow tube.

The temperature in the H_2 chamber is determined with a carbon glass resistor. The temperature T_1 is electronically regulated using standard techniques and has fluctuations averaged over 3 s of $< 5\,\mu$K. The overall error in determining $\Delta T = T_2 - T_1$ is about 50 μK.

Appropriate combinations of the fountain pump and counterflow heater allowed different regions of the (v_n, v_s)-plane to be explored, as will be described in §8.1.

4.2. *Second and temperature-difference measurements in a wide channel*

Pure counterflow measurements in a channel 1 cm × 1 cm × 40 cm have been pursued by the Oregon group for about 10 years. The advantage of a wide channel is that second sound transducers can be installed to measure the attenuation of second sound

owing to the vortices. The disadvantage is that the effective thermal conductivity of the fluid is so large because of the superfluidity that it is difficult to measure the temperature gradient.

An unwelcome difficulty arose in the early designs (Cromar 1977) when it was determined that the vortex line density was not axially homogeneous, but decreased away from the heater. A new channel was designed and built which exhibits axially homogeneous line density, probably because of the effort made to produce a uniform, leak-free heater source. The channel is constructed of interchangeable units joined by indium o-ring seals, into some of which we can insert second sound transducers or thermometers (for details, see Barenghi 1982; Swanson 1985). One possible arrangement of the channel is shown schematically in figure 5. Figure 6 is a photograph of the rotating table upon which the channel is mounted.

The heater is a nichrome film deposited on a fused quartz substrate, joined by indium seals to the channel. Electrical contact to the nichrome is through superconducting indium along two opposite edges, providing a uniform current density. The heat capacity of the film is very low and hence can respond very rapidly to pulsed inputs.

The transverse second sound transducers are capacitor loudspeakers and microphones with Nuclepore membranes. The membranes have many 0.1 μm holes, allowing ready passage of superfluid but nearly no passage of normal fluid; membrane oscillations create counterflowing oscillations of the normal and superfluid, i.e. second sound. For details of their behaviour, see Giordano (1984*a*,*b*), Giordano & Musikar (1984), and references therein. Line densities determined by propagation in the transverse direction are called L_T.

The axial attenuation of second sound is measured by transducers at the bottom of the channel, and line densities determined from this are called L_A. The transmitter was made of electrical resistance board, and the receiver was a Nuclepore transducer described above. The resistance board is able to produce a powerful low-frequency burst of second sound needed to traverse the long axial path in the presence of high vortex line densities.

Second sound attenuation can be determined by the width of a resonance peak or the decay of echoes of a second sound burst. We find the two methods agree to better than 2 %. The best line density resolution we can currently achieve is about 20 cm^{-2} over a range of 0–200000 cm^{-2}, a factor of 50 better than we could obtain 9 years ago (Cromar 1977).

Axial temperature difference measurements are made by using two germanium resistance thermometers mounted 30 cm apart on the sidewalls, forming two legs of an impedance bridge. The thermometers are matched (i.e. their resistances as a function of temperature are nearly the same) so that correlated temperature fluctuations (i.e. bath temperature fluctuations) cause only a small second-order effect in temperature-difference measurements. Temperature gradients smaller than 10^{-8} K/cm could be determined in this way.

4.3. *Ion measurements in a wide channel*

Another tool which has been profitably used is the interaction of ions in liquid helium with vortices (Donnelly & Roberts 1969). Negative and positive helium ions can be produced in helium II by various means such as radioactivity and field emission. Negative ions are relatively large ($R \approx 16$ Å) bubbles cut out of the liquid owing to the repulsive electron–helium atom interaction. Positive ions are smaller ($R \approx 6$ Å) solid objects held together by electrostrictive forces. In the vicinity of a vortex line

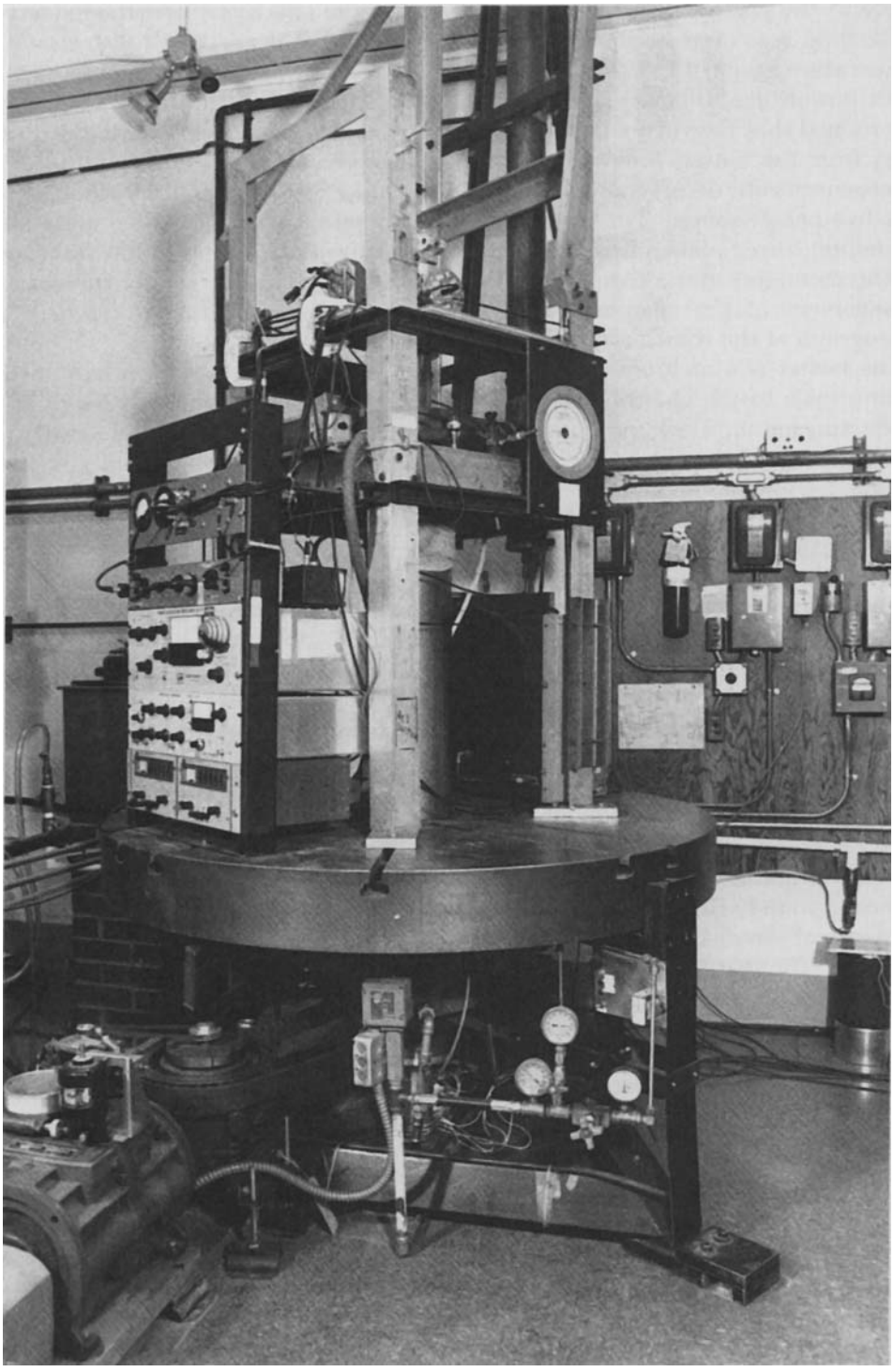

FIGURE 6. The quantum turbulence apparatus at the University of Oregon mounted on the 54 inch rotating table. The channel is contained in the metal dewar flask mounted on the centre of the table.

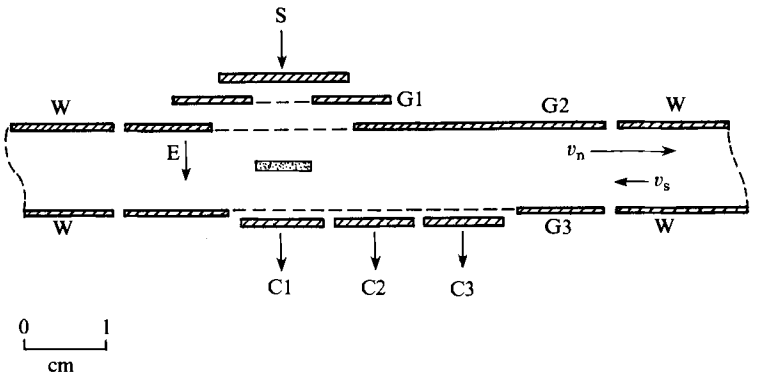

FIGURE 7. Apparatus designed by Awschalom *et al.* (1984) to study the distribution of line density and normal fluid velocity in a counterflow. S is a tritium source to produce ionization, G1, G2, and G3 are pulsed grids with associated guard plates, C1, C2 and C3 are collectors, W is the grounded channel wall. The dotted region represents a typical charge pulse, and extends 0.8 cm into the plane of the figure.

an ion does not experience any drag owing to the circulating superfluid, but it does experience the radial pressure drop associated with the potential flow about the vortex. Both species of ions are pushed into the vortex core, the negative ions more strongly. The result is that at temperatures above 1 K (which is the range of interest of our discussion) positive ions do not remain trapped owing to thermal fluctuations. Negative ions remain trapped up to a 'lifetime edge' of about 1.7 K, forming a useful probe of quantum turbulence.

Awschalom, Milliken & Schwarz (1984), have used pulsed ion techniques to study the vortex-line length density distribution and normal fluid velocity field in turbulent counterflow. This technique was previously used by Schwarz & Smith (1981) (see §8.3). Their apparatus is shown in figure 7. An ion source and a variety of interchangeable grid and collector assemblies are built into the channel walls. In a typical measurement, a narrow pulse of negative ions is gated into the channel and allowed to propagate to a particular position under the action of a drift field E. The field is then switched off, allowing the pulse to remain at this position for as long as several seconds. Some of the ions in the pulse are trapped by quantized vortices at a rate determined by the local value of the line density L; the rest drift along with the local normal fluid velocity v_n. Later, E is turned back on and the received pulse is measued by means of one or more electrometers as it arrives at the collectors. From the amplitude of the observed pulse and where it falls on the collectors, local values of L and v_n can be readily determined as a function of where the pulse was stopped. The spatial resolution achieved with this interrupted flight technique is better than 1 mm.

4.4. *A chemical potential detector*

Yarmchuck & Glaberson (1979) have developed a device to make direct measurements of chemical potential differences. This is a fundamentally important measurement because the chemical potential indicates that dissipation is occurring, and is a direct measurement of the rate at which quantized vortices change the phase of the order parameter (Anderson 1966). The device, shown in figure 8, consists of a differential pressure transducer connected via superleaks to the measurement regions. The superleaks (ideally at least) allow no chemical potential difference along them, and have infinite thermal resistance. The copper heat exchanger connecting the input

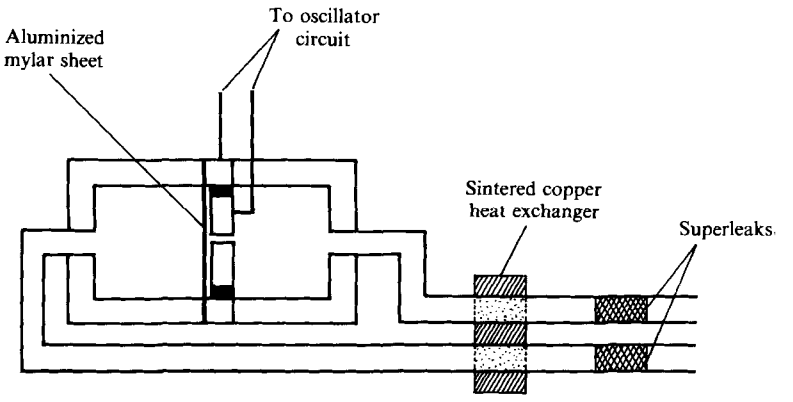

FIGURE 8. The chemical potential detector of Yarmchuck & Glaberson (1979). The two superleak outlets are connected to the positions between which the chemical potential difference is to be measured.

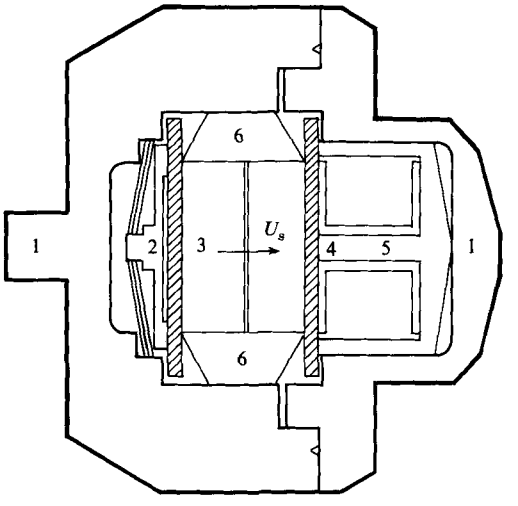

FIGURE 9. Thermal shock wave apparatus built at the California Institute of Technology. The operation is described in the text.

tubes ensures that the temperature difference between the two sides is near zero, converting $\Delta\mu$ to a pressure difference (see (2.18)). This pressure difference bows an aluminized Mylar membrane whose displacement is detected by the change in capacitance between the membrane and a fixed metal plate.

The chemical potential detector has been incorporated into other modern apparatus, for example Lorenson *et al.* (1985) (see §5.11).

4.5. *Shock-wave apparatus*

Second sound shock waves form an interesting, but perhaps underused, probe of quantum turbulence. In §8 we describe some shock-wave experiments, so we include a brief description of the apparatus here.

A gasdynamical cryogenic shock tube for liquid helium research was developed by Liepmann, Cummings & Rupert (1973) and Cummings (1974). A shock wave is produced in the helium vapour above the bath by modified standard techniques and

allowed to strike the free surface of the bath, producing both a pressure and a temperature shock in the liquid helium II.

Temperature shock waves without significant accompanying pressure shock waves can be produced easily by the rapid heating of a thin conducting film. A series of such tubes have been constructed by Liepmann's group (Liepmann & Laguna 1984). One of these is shown in figure 9. Part 1 is a brass housing for the apparatus, 2 is a spring loading for the heater, a 1000 Å thick nichrome film, vacuum deposited on a quartz substrate, 3. The sensor, 4, separated from the heater by spacer 6, is a thin film of superconducting material biased to be at its transition field by a superconducting magnet, 5. Such a biased superconducting film has a very fast and sensitive response to heat pulses. The shock-wave tube is made of Teflon.

5. Survey of counterflow induced turbulence phenomena

This section is a discussion of the properties of quantum turbulence generated by steady heat flux in a uniform channel. Much of what is said applies to more general counterflow situations (divergent or unsteady heat flux or non-zero mass flux), but there are enough differences and complications that we will defer a brief discussion of some more general flows to §8 below.

5.1. *Critical heat flux*

Vinen (1958) observed that a critical heat flux, and hence a critical average counterflow velocity v_c is necessary to generate an observable quantity of vortex line. He did this with second sound attenuation, and the existence of a critical counterflow velocity has been confirmed since by second sound attenuation, temperature and chemical potential gradients, as well as ion trapping (Tough 1982).

5.2. *Dependence of line density on counterflow velocity*

The dependence of the average line L_0 upon v_{ns} near critical is complicated. But observers generally agree that beyond the critical region

$$L_0 \approx \gamma^2(v_{ns}-v_0)^2, \tag{5.1}$$

where γ and v_0 are functions of temperature. The precise values of γ and v_0 have been the subject of controversy (Barenghi, Park & Donnelly 1981), but the turbulent state classification of Tough (1982) described in §5.9, the recent work on scaling (Schwarz 1982*b*; Swanson & Donnelly 1985) described in §6, and the measurement of the tangle anisotropy described in §5.6 combine to resolve the experimental discrepancies.

5.3. *The Gorter–Mellink law*

The temperature gradient is proportional to the cube of the heat flux when well beyond critical. This relationship, named the Gorter–Mellink law, is approximately obeyed at temperatures well below T_λ, but in general it needs to be modified, as described in §6.2.

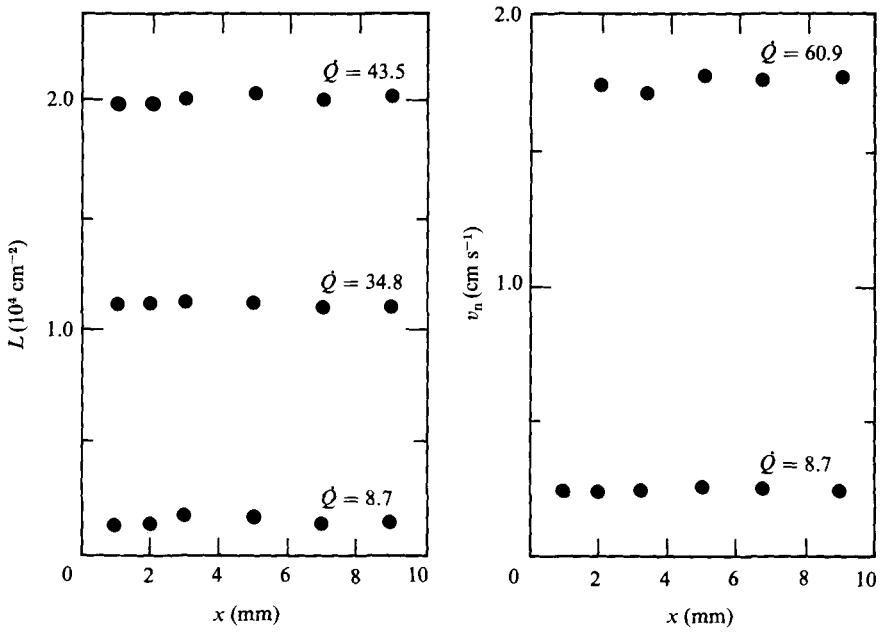

FIGURE 10. Data of Awschalom *et al.* (1984) on the transverse homogeneity of (*a*) the line density (*b*) the normal velocity v_n.

5.4. *Axial homogeneity of vortex line density in a counterflow channel*

The vortex line density in turbulent counterflow is axially homogeneous in a properly designed channel (see §4.2). The axial homogeneity is consistent with the Vinen equations which imply that the tangle is sustained by the local value of v_{ns}. Further evidence for local creation has been provided by shock-wave experiments of Barenghi (1982) described in §8.5.

5.5. *Transverse homogeneity of line density and normal fluid velocity*

Awschalom *et al.* (1984) have reported that the vortex line density L is independent of transverse position over at least 80 % of a channel of width 1 cm. This observation was made by ion trapping in an apparatus described in §4.3. In the same experiment, it is reported that the normal fluid velocity profile is uniform over at least 80 % of the channel and the normal fluid is certainly not in Poiseuille flow. The data are shown in figure 10(*a*,*b*).

5.6. *Anisotropy of the tangle*

The standard assumption since the work of Vinen (1957*a*,*c*) has been that the vortex line density is isotropic. We find by simultaneous transverse and axial measurements that the line density distribution is substantially flattened in a direction perpendicular to the axial flow (Wang, Swanson & Donnelly 1986). Figure 11 shows the ratio L_T/L_A (see §4.2), which would be unity for an isotropic distribution and 0.5 if all of the lines were perpendicular to the flow.

5.7. *Drift of the tangle*

Vinen (1957*c*) assumed that the vortex lines, being an excitation of the superfluid. would have velocity v_s and thus move toward the heater. Measurements by Ashton & Northby (1975) suggested that the average line velocity $v_L = fv_n$ where

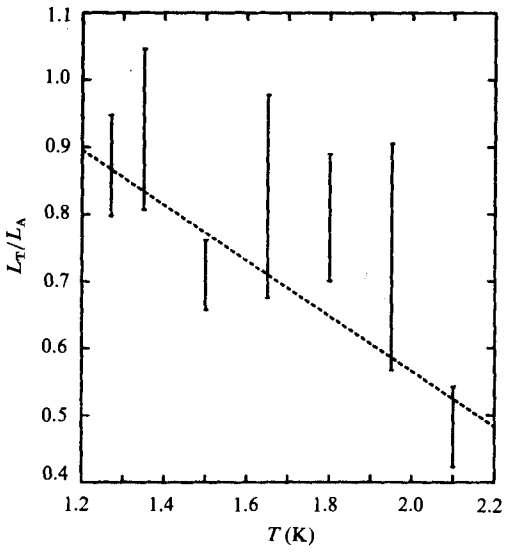

FIGURE 11. The ratio of L_T/L_A of line density as a function of temperature (Wang *et al.* 1986). Even with the substantial uncertainties (which represent three standard deviations), it is evident that the tangle is not isotropic since L_T/L_A is not unity.

$0.2 < f < 0.3$ (for 1.3 K $< T <$ 1.6 K), suggesting that the tangle moves toward the exit of the channel. More recent ion measurements by Awschalom *et al.* (1984) concluded by finding $f < 0.1$ (at 1.45 K). Barenghi *et al.* (1983) suggested that combined temperature gradient and second sound measurements could yield the ratio $|\langle \boldsymbol{v}_L - \boldsymbol{v}_s \rangle| / |\langle \boldsymbol{v}_n - \boldsymbol{v}_s \rangle| = v_{Ls}/v_{ns}$. This measurement was carried out by Wang *et al.* (1986), who found $v_L \approx v_s$ (for temperatures from 1.27 to 2.1 K), in accord with Vinen's original assumption (see figure 12).

5.8. *Fluctuations*

The first apparent observation of intrinsic fluctuations of the tangle were reported by Hoch, Busse & Moss (1975) and Mantese, Bischoff & Moss (1977). Further measurements were reported by Ostermeier *et al.* (1980), and Smith & Tejwani (1984). Since then apparatus and detection capability has improved considerably and some doubt has arisen about the exact interpretation of these early measurements. For example, the drift of the tangle past a detector will itself produce fluctuations. The intrinsic fluctuations should reflect the dynamics of the tangle itself, and probably the size of the volume probed. On the other hand, the Vinen equations can be interpreted in a way which gives the response to induced fluctuations of v_{ns}. An experiment to test this prediction by Barenghi, Swanson & Donnelly (1982) fully confirms the predictions of Vinen's equations.

5.9. *Tough classification of turbulent states*

Tough (1982) has analysed the vast quantities of steady, uniform counterflow data and found that there is one feature of the channel geometry which is crucial in determining the phenomena, the cross-sectional aspect ratio. (Apparently the channels used are long enough for the length to width ratio to be of little importance, at least well beyond critical.) For low-aspect-ratio channels (e.g. nearly square or circular) there are two turbulent states, state TI at low heat fluxes and state TII

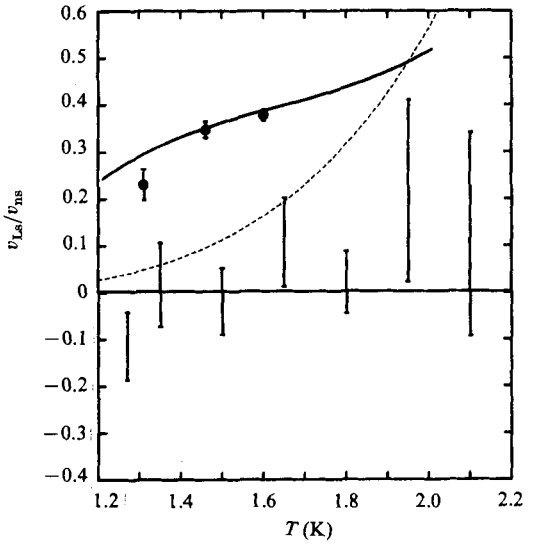

FIGURE 12. The ratio v_{Ls}/v_{ns} as a function of temperature. The bars represent the data of Wang *et al.* (1986) (the range shown is three standard deviations). The solid horizontal line represents a fit to these data. The data of Ashton & Northby (1975) are shown as bars with circles and the simulations by Schwarz (1978) as the solid curved line. The dashed line is the laboratory rest frame.

at high heat fluxes, which are separated by a rather complicated transition (see §5.11) and have different characteristic values of γ. For high-aspect-ratio channels there is only one turbulent state, state TIII, which has values of γ similar to state TII. Tough also designated the turbulence in pure superflow as state TIV, a state which has mass flow and presumably a flat velocity profile. From the latest data (Opatowsky & Tough 1981) it appears that γ in state TIV agrees quantitatively with γ in state TII (see Awschalom *et al.* 1984 figure 1*b*).

5.10. *Combined rotation and counterflow*

Combined rotation and heat flow is a relatively new area of investigation. Measurements at Oregon (Swanson, Barenghi & Donnelly 1983) appear to be relatively simple in two limits:

(i) Limit of large line density L_H due to heat, slow rotation. Here the effect of rotation is not simply to add line density $L_R = 2\Omega/K$. Instead the tangle is polarized to accomplish the rotation. The effective polarization increases with rotation Ω by analogy to a gas of magnetic dipoles in a magnetic field. The results scale with L_R/L_H by analogy to $\mu H/kT$. Thus rotation appears to produce alignment in the tangle, as does a magnetic field, and L_H appears to play the role of a disordering heat bath in the statistical mechanics of quantum turbulence.

(ii) Limit of fast rotation and small axial heat flux. Any rotation eliminates the critical velocity v_c. In this limit two critical counterflow velocities appear, v_{c1} and v_{c2}, which scale as $\Omega^{\frac{1}{2}}$. The first appears to correspond to the Donnelly–Glaberson instability (Cheng, Cromar & Donnelly 1973; Glaberson, Johnson & Ostermeier 1974): excitation of helical waves by the counterflow on the vortex lines induced by rotation. The second appears to be a transition to turbulence, with the rotation induced array becoming a vortex tangle.

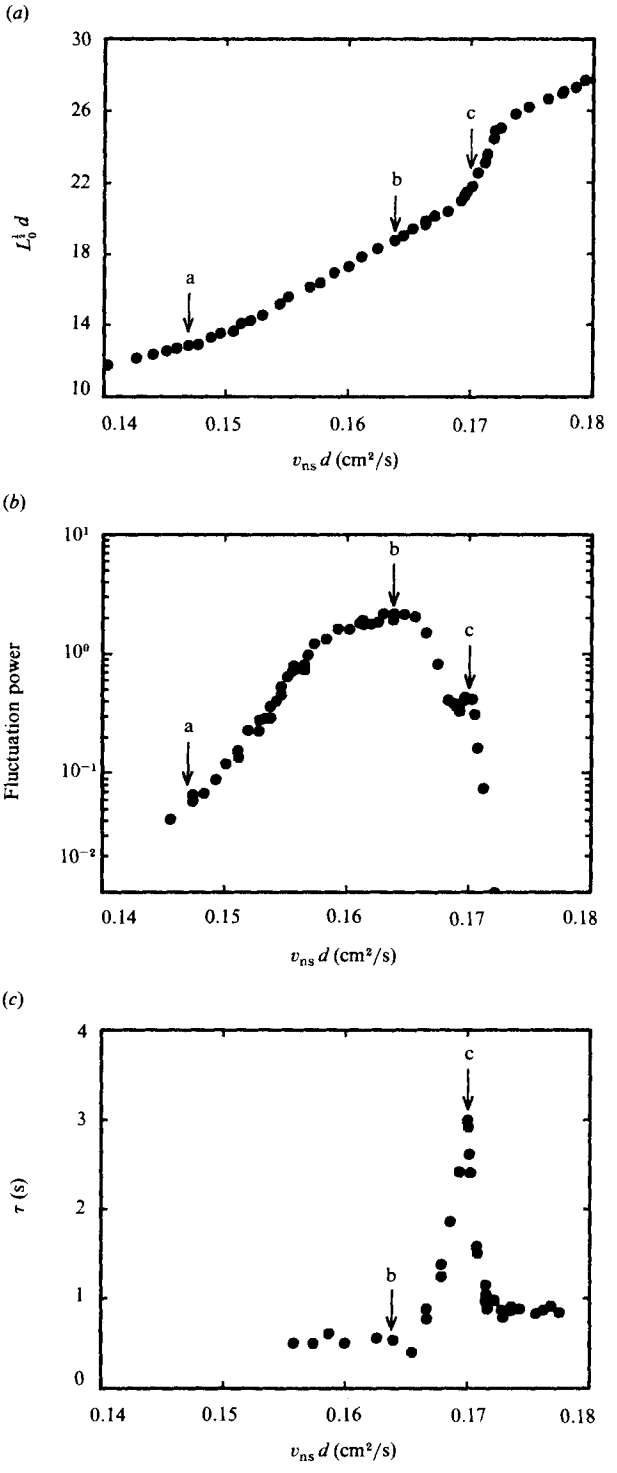

FIGURE 13. Data of Lorenson *et al.* (1985) on the dynamics of the TI–TII transition. The data, plotted as a function of $v_{ns}\, d$ to remove most of the channel size dependence, are (*a*) dimensionless line density, (*b*) fluctuation power around 1 Hz, and (*c*) the response time. Points *a*, *b*, and *c* are described in the text.

5.11. *Dynamics of the TI–TII transition*

The TI–TII transition is most easily observed in narrow channels. Recently Tough's group have reported complex dynamical features of this transition (Lorenson *et al.* 1985), made by measuring the chemical potential difference $\Delta\mu$ across a short (1 cm), narrow glass tube (diameter 0.0134 cm). The narrowness of the tube increases $\Delta\mu$ for a given state, while the shortness decreases the steady difference but emphasizes the fluctuations. The measurements of $\Delta\mu$ were made with a device similar to that of Yarmchuck & Glaberson described in §4.4 above, and the line density can be deduced as described in §2.6. The results, shown in figure 13, depict a rich and complicated transition. Figure 13(*a*) shows the steady state line density (note that $L_0^{\frac{1}{2}}d$ is essentially the number of vortices across the flow tube), and it is clear that the transition is relatively wide. Point *a* corresponds to the start of the region where L_0 differs from state TI. The fluctuation spectra are relatively featureless, but the power spectral density around any particular (fairly low) frequency changes dramatically through the transition, as shown in figure 13(*b*), with a broad peak around point *b* and a peculiar subpeak at point *c*. Figure 13(*c*) shows that point *c* corresponds to a sharp peak in the response time, which is otherwise relatively steady. This system presents the exciting prospect of a continuous transition in which the fluctuations can be studied directly.

6. Vortex dynamics and scaling

6.1. *The conditions for geometric similarity*

The classical vortex dynamics of an ideal fluid and the theory of mutual friction combine to give an equation of motion for a vortex filament in a direction transverse to its local tangent (this derivation is given, for example, by Swanson & Donnelly 1985). The theory underlying vortex dynamics in helium II is primarily the work of Hall & Vinen (1956*b*). Schwarz (1978) has put the equations in a quite useful form and has given a dimensionless form of vortex dynamics, from which he derived a scaling law (Schwarz 1982*b*). The discussion below is a summary of that in Swanson & Donnelly (1985), whose work made use of Schwarz (1982*b*) and Awschalom *et al.* (1984).

In the approximation that the vortex core has no inertia, the dimensionless line velocity in the superfluid frame, $\boldsymbol{u}_{\mathrm{L}} = (\boldsymbol{v}_{\mathrm{L}} - \boldsymbol{v}_{\mathrm{s}})/v_{\mathrm{ns}}$, can be written as

$$\boldsymbol{u}_{\mathrm{L}} = \boldsymbol{u}_{\mathrm{i}} + \alpha \boldsymbol{s}' \times (\boldsymbol{u} - \boldsymbol{u}_{\mathrm{i}}) - \alpha' \boldsymbol{s}' \times (\boldsymbol{s}' \times (\boldsymbol{u} - \boldsymbol{u}_{\mathrm{i}})), \tag{6.1}$$

where $\boldsymbol{s}' = \boldsymbol{\kappa}/|\boldsymbol{\kappa}|$ is the unit tangent to the line, $\alpha = B\rho_{\mathrm{n}}/2\rho$, $\alpha' = B'\rho_{\mathrm{n}}/2\rho$, and we have defined the dimensionless counterflow velocity $\boldsymbol{u} = \boldsymbol{v}_{\mathrm{ns}}/v_{\mathrm{ns}}$ and tangle-induced superfluid velocity $\boldsymbol{u}_{\mathrm{i}} = \boldsymbol{v}_{\mathrm{i}}/v_{\mathrm{ns}}$. Time will scale with d/v_{ns}, where d is a typical flow-channel dimension.

Dynamical similarity in two geometrically similar flows requires that all tangle lengths scale with d and that the velocity ratio $\boldsymbol{u}_{\mathrm{i}}$ must be the same for similar points on the tangles in each flow. Since the core parameter a cannot scale with d (remaining fixed with temperature), the finite core size a becomes important for scaling, a fact not appreciated until recently (Schwarz 1982*b*; Swanson & Donnelly 1985). Approximate dynamical similarity will occur if u_{i}, the average magnitude of $\boldsymbol{u}_{\mathrm{i}}$, is the same in the two flows.

Using the localized induction approximation of Arms & Hama (1965) one finds that $\boldsymbol{u}_{\mathrm{i}}$ is proportional to a logarithmic factor $l = \ln(R/a_{\mathrm{eff}})$, where R is the local radius

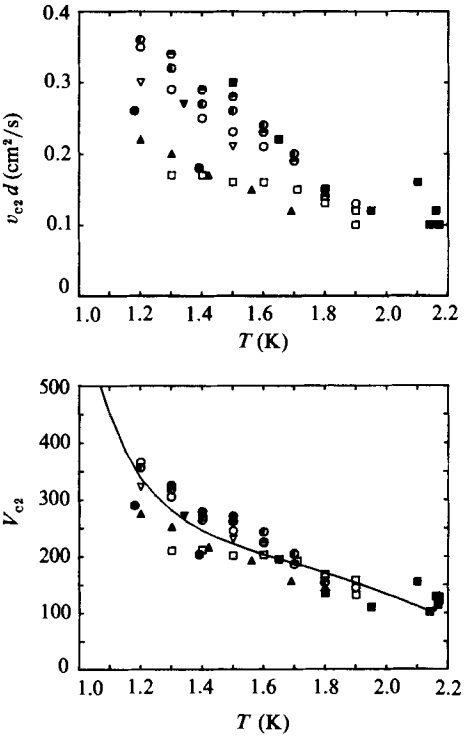

FIGURE 14. Second critical velocity in small-aspect-ratio channels at various temperatures. The left-hand plot is scaled with channel size, while the right-hand plot includes the logarithmic parameter as in (6.4). d (cm): ■, 1.00 Swanson (1985); ▼, 0.262 Chase (1963); ◓ 0.159 Chase (1963); ◐, 0.140 Peshkov & Tkachnko (1961); ○, 0.080 Chase (1962); ▽, 0.057 Oberly & Tough (1972); ●, 0.0366 Brewer & Edwards (1961); □ 0.0131 Ladner, Childers & Tough (1976); ▲, 0.0108 Brewer & Edwards (1961).

of curvature of the line and $a_{\rm eff}$ is an effective core parameter. In terms of the average line density L_0, $u_{\rm i}$ will be proportional to the average logarithmic factor

$$l_0 = \ln\left(\frac{1}{acgL_0^{\frac{1}{2}}}\right) \approx -\ln\left(aL_0^{\frac{1}{2}}\right), \tag{6.2}$$

where c and g are of order one ($c = \langle 1/R\rangle/L_0^{\frac{1}{2}}$ and $g = a_{\rm eff}/a$; see Schwarz 1978 for calculations of c from simulations). Defining $\beta = \kappa l_0/4\pi$ (with dimensions of kinematic viscosity), the dimensionless applied counterflow velocity V (analagous to a Reynold's number) upon which tangle properties will depend is

$$V = \frac{v_{\rm ns}\,d}{\beta} = \frac{L_0^{\frac{1}{2}}\,cd}{u_{\rm i}}. \tag{6.3}$$

6.2. *Implications of scaling*

There are two major implications of the scaling of tangle properties with V, i.e. the scaling of critical velocities with channel size and the relationship between line density and counterflow velocity (for high velocities). This relationship has further implications, e.g. the scaling of γ with channel size and the temperature and heat flux dependence of the Gorter–Mellink law exponent.

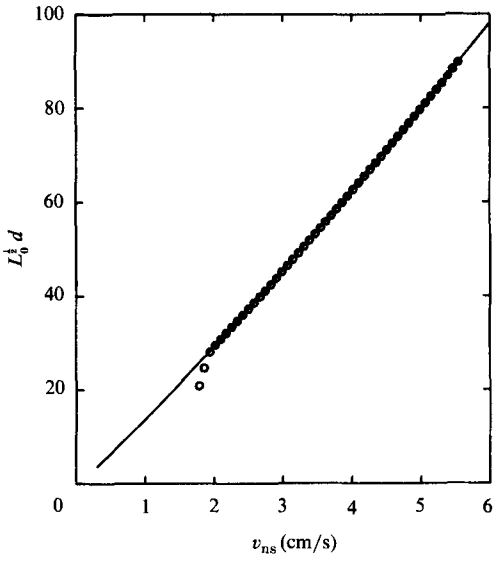

FIGURE 15. $L_0^{\frac{1}{2}}d$ as a function of v_{ns} at 1.7 K. The data are from Martin & Tough (1983). The line represents (6.5) with $cg = 3$ and $u_i/c = 0.17$.

We can define a dimensionless critical velocity from (6.4):

$$V_c \equiv \frac{v_c d}{\beta_c}, \tag{6.4}$$

where v_c and β_c are the values of v_{ns} and β at the critical velocity. In figure 14 we show measurements of $v_{c2}d$, the second critical velocity in small aspect ratio channels scaled by the channel size (ignoring the logarithmic parameter), and of V_{c2}, i.e. the same data scaled according to (6.4). We can see substantial improvement in agreement between measurements in various sized channels with the inclusion of the logarithmic parameter. Similar improvements in agreement can be seen for other critical velocity measurements (Swanson & Donnelly 1985).

At high counterflow velocities, the boundary region becomes less important for determining average tangle properties, and L_0 need not be proportional to d^{-2}. Then (6.3) can be written as

$$L_0^{\frac{1}{2}} = \frac{u_i}{\beta_c} v_{ns}. \tag{6.5}$$

The dependence of L_0 on v_{ns}^2 can thus be derived simply from the scaling of vortex dynamics in the approximation that the logarithmic parameter is constant. Inclusion of the logarithmic parameter gives a remarkably good fit to the data, as can be seen in figure 15.

We can make a linear approximation of (6.5) about some $v_{ns} = v_{ns0}$, where l_0 has the value l_{v0}, finding

$$L_0^{\frac{1}{2}} = \gamma(v_{ns} - v_0), \tag{6.6}$$

where $\gamma = 4\pi u_i/\kappa c(l_{v0} - 1)$ and $v_0 = v_{ns0}/l_{v0}$. The parameter v_0 which appears in this expression for L_0 is the same as the v_0 appearing in the Gorter–Mellink relationship. It has no physical significance. Its presence arises naturally due to logarithmic scaling, and its value depends on where one makes the linear approximation as well as on temperature and channel size. Below we will use a nonlinear power law

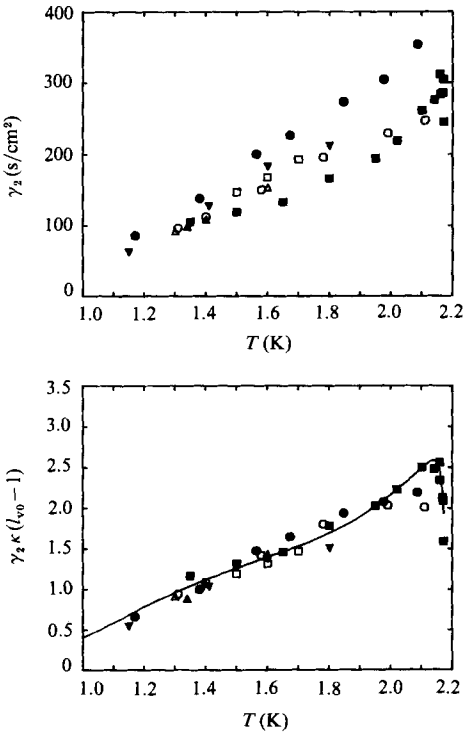

FIGURE 16. γ_2 as a function of temperature measured by various investigators. The upper plot shows γ_2 and the lower plot shows γ_2 scaled by the implicit channel-size dependence. ■, 1.00, Swanson (1985); △, 0.318 Dimotakis & Broadwell (1973); ▲, 0.240 Vinen (1957*a*); ○, 0.140 Peshkov & Tkachenko (1961); □, 0.100 Martin & Tough (1983); ▼, 0.080 Chase (1962); ●, 0.0366 Brewer & Edwards (1961).

approximation to (6.5), $L_0^{\frac{1}{2}} = bv_{\rm ns}^{\rm n}$, which is good over a much wider range than the linear approximation.

It is clear from comparing (2.25) with (6.5) that the quantity γ is a function of the logarithmic parameter, which is implicitly a function of $v_{\rm ns}$. In experiments measuring γ the counterflow velocity is usually somewhat above critical, so the implicit velocity dependence of γ is seen as a channel size dependence. Figure 16 shows γ_2 (γ in state TII) as measured by various investigators, and the same measurements scaled by the implicit channel size dependence of γ. We see substantial improvement in the agreement. Similar improvements in agreement can be seen for other measurements of γ.

The logarithmic parameter also has implications for the Gorter–Mellink relationship between the temperature gradient and the applied heat flux,

$$\nabla T_{\rm T} = -\frac{F_{\rm ns}}{S\rho_{\rm s}} \propto q^m. \tag{6.7}$$

If (2.11) held, then m would be three, which is only very roughly correct. It can be shown (Swanson 1985) that

$$F_{\rm ns} = -\rho_{\rm s}\kappa G\alpha L v_{\rm ns}, \tag{6.8}$$

where G is a geometric factor ($G = \frac{2}{3}$ if the tangle is isotropic and drifting with the superfluid). Equations (6.7), (6.8), and the power law approximation to (6.5) combine to yield (6.7) with $m = 2n+1$. Including the velocity dependence of α (or equivalently

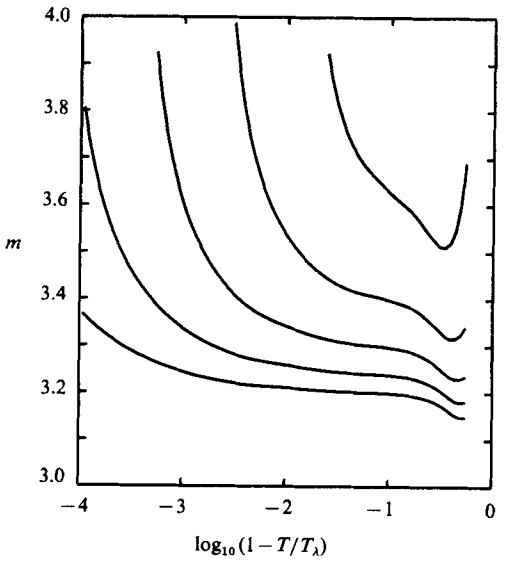

FIGURE 17. The Gorter–Mellink m as a function of temperature and heat flux. From the top the lines are for heat fluxes of 10 W/cm^2, 1 W/cm^2, 0.1 W/cm^2, 10 mW/cm^2, and 1 mW/cm^2.

B in (2.12)), one finds that (6.7) is a good local approximation about some heat flux q_0, with m a function of temperature and q_0 as shown in figure 17. These values are consistent with a variety of experiments (Ahlers 1969; Bon Mardion, Claudet & Seyfert 1978; Swanson 1985) that have roughly determined m. The theory leading to this figure breaks down as m grows, essentially because the core becomes comparable to $L_0^{-\frac{1}{2}}$, but it is probably good while m is less than 4.

It can be seen from this section that the logarithmic parameter, the logarithm of the ratio of a macroscopic tangle length to the atomic sized core parameter, has effects of macroscopic and even engineering consequences. Apparently the one-dimensional nature of the tangle makes this ratio more important at larger values than say, for example, the ratio of a container dimension to the mean free path in kinetic theory.

7. Simulations of vortex dynamics

The dynamics of vortices in helium II forms a particularly attractive problem to simulate numerically. The equations of motion are well known and, because of the microscopic core size, a thin vortex filament approximation is very good. One needs to follow only a one-dimensional set of points moving in three-dimensional space, rather than a three-dimensional set as in, for example, simulations of the Navier–Stokes equation. In addition, Arms & Hama (1965) developed a simple local approximation to the vortex line induced velocity which is very useful in helium II. Despite this attractiveness, significant simulations of quantum turbulence have been carried out only by Schwarz (1978, 1982*b*, 1983, 1985) at IBM over a number of years. We will discuss in this section what we feel are the major insights for quantum turbulence from the IBM simulations, and what are the outstanding discrepancies with experiment.

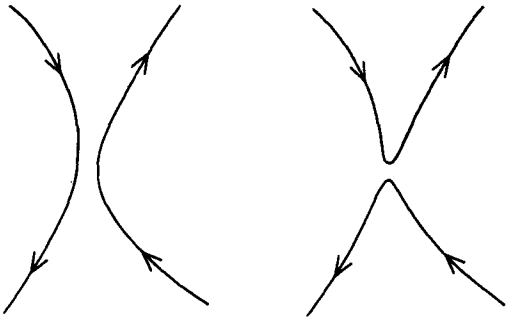

FIGURE 18. Illustration of a possible reconnection sequence between vortex filaments in a tangle.

7.1. *Major insights from the simulations*

Schwarz (1978) has shown that the Arms–Hama local induction approximation (hereafter referred to as the local approximation) is generally valid in quantum turbulence, but that there are some instances when the 'far field' becomes important. These instances occur when previously distant portions of the tangle or the tangle and its image approach more closely than a critical distance (Schwarz 1985). Thus vortex simulations can be successfully broken down into two parts:

(i) A local approximation which is generally valid.

(ii) Discrete events, line–line or line–boundary 'crossings', where the far field is significant.

With a local approximation, portions of the tangle with small radius of curvature or local induced velocity v_i opposite to the counterflow will evanesce due to mutual friction. Other portions will grow and be annihilated at the walls. Thus vortex crossings are necessary to keep a tangle self-sustaining, and the treatment of such crossings is crucial to a successful simulation. In early work, Schwarz (1978) forced a randomization of the vortex configuration in the vicinity of the crossing, which was costly in computer time, but allowed successful simulations of steady-state flows without boundaries.

A second major insight from Schwarz's work (1982*b*) is that one can replace the configuration randomization with a simple 'topology-changing reconnection', with similar results and a great increase in ease of implementation. Such a reconnection is depicted in figure 18. In recent work, Schwarz (1985) has shown that a reconnection is feasible, but classical vortex dynamics breaks down as the distance of closest approach becomes of the order of the core size, and one is left with a quantum mechanical problem. There is some evidence (Schwarz 1982*a*) that, in fact, a topology changing reconnection does not occur at every crossing. What really happens at a crossing is a major unsolved problem in quantum turbulence, which we shall discuss further in §7.3.

Probably the greatest lesson from Schwarz's simulations is the success in reproducing experimental phenomena which has been achieved using the equations of vortex dynamics with several simplifying assumptions. The counterflow was assumed to be uniform, as in state TIV (pure superflow), the velocity dependence of α and β was ignored (eliminating the weak velocity dependence of L_0/v_{ns}^2), α' was ignored (valid except near T_λ), and periodic boundary conditions were used (ensuring homogeneity of the line density).

In early simulations (Schwarz 1978), i.e. prior to implementing the reconnection

ansatz, boundaries were ignored and thus critical velocities were not reproduced. Nevertheless, the success was quite remarkable. The v_{ns}^2 dependence of L_0 was reproduced (as scaling arguments now show must happen). The mutual friction force and the line density were in suprising quantitative agreement with experiment, well within the range of the rather scattered experimental results of the time (see §5.2). The simulation produced a drift velocity of the tangle as a whole which agreed with the data of Ashton & Northby (1975) (although current experimental results contradict this result; see §5.7).

Implementation of the topology changing reconnection ansatz allowed boundaries to be included through line–boundary reconnections (although $\boldsymbol{v}_{ns}$ remained uniform). With this improvement, Schwarz (1983) was able to reproduce v_{c1} and v_{c3}, the first critical velocities in small- and large-aspect-ratio channels. It is curious that the temperature dependence of the critical velocity found by the simulations was much stronger than v_{c4} (Baehr, Opatowsky & Tough 1983), and indeed similar to that in counterflow. Awschalom *et al.* (1984) report new calculations of γ (smaller than reported by Schwarz 1978) which agree remarkably well with the measurements of γ_2 and with the most recent measurements of γ_4 (Opatowsky & Tough 1981).

7.2. *Current discrepancies with experiment*

The closest experimental approximation to the uniform flow used in numerical simulations is pure superflow. The current discrepancies of simulations and experiment are (counterflow observations are included if pure superflow data is not contradictory):

1. The transverse homogeneity of the vortex line density has not been reported in the case where boundaries were considered.
2. The anisotropy of the tangle observed in state TII has not been reported.
3. The drift velocity has not been reported in the later simulations.
4. The later simulations produce critical velocities comparable to those observed in states TI and TIII and not in TIV as might have been expected (Baehr *et al.* 1983).
5. The aspect ratio dependence of the critical velocity seen in simulations has not been observed in pure superflow.

7.3. *Vortex reconnections: a problem in quantum mechanics*

The idea of vortex reconnections was first put forward by Feynman (1955) in his discussion of the decay of a vortex tangle into heat. When two oppositely-directed bits of vortex line approach closely enough, one might speculate that the reduction in the scale of the flow might cut off the circulation and hence allow the reconnection process to occur without violation of Kelvin's circulation theorem. This problem has not been directly addressed, and is likely to be a difficult problem in quantum mechanics. Some indirect evidence, however, exists. Jones & Roberts (1982) have made a study of the Ginzburg–Pitaevskii equation for a family of vortex rings of steadily decreasing ratio of radius to core size. They find that at a definite value of this quantity, the circulation disappears, and the remnant of the vortex becomes solitary waves of compression. In the most recent paper on motions in a Bose condensate, Jones, Putterman & Roberts (1986) have demonstrated by direct numerical calculation the establishment of a vortex core and circulation in the evolution of the nonlinear Schrodinger equation.

The Schwarz simulation has gone beyond the Feynman speculation in addressing the problem of a self-sustaining tangle. In particular he has shown that when bits of line approach which are parallel in sense of circulation, the line can wrap around

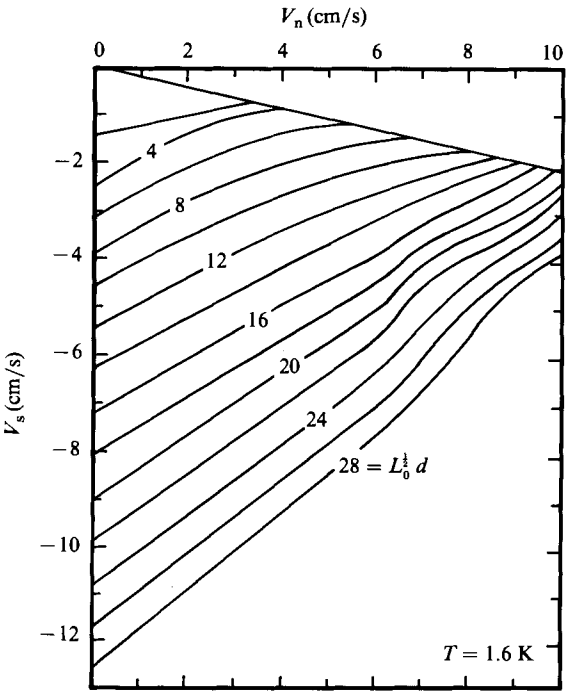

FIGURE 19. Contours of constant line density L_0 (shown as $L_0^{\frac{1}{2}}d$) in the (v_n, v_s)-plane at 1.6 K (Baehr & Tough 1985).

in such a way as to allow reconnection to take place. The final resolution of the quantum mechanics is a challenging problem, but at the present time it looks as if the necessary conceptual basis is given by the Jones & Roberts calculation.

8. Investigations of more general flows

8.1. *Pipe flow with mass flux*

The bulk of the results discussed in this paper, and indeed in the literature as a whole, have to do with pure counterflow, a state of zero mass flux (equation (2.3)). In counterflow it is known (Tough 1982) that the dissipation depends qualitatively on the tube shape. In tubes of square or circular cross-section, the turbulence evolves from a low density state TI to a high density TII as the counterflow is increased. High-aspect-ratio channels are in state TIII. Pure superflow, state TIV, has dissipation independent of tube shape.

Using the apparatus described in §4.1 it is possible to add a counterflow to a superfluid flow at various selected velocities. In this way dissipation can be mapped out in the (v_n, v_s)-plane for many velocity combinations between pure superflow and counterflow. Early experiments of this type were reported by investigators at Leiden, most recently in van Beelen's group (e.g. Slegtenhorst, Marees & van Beelen 1982).

An investigation by Baehr & Tough (1985) examines the dissipation in detail in a quadrant of the (v_n, v_s)-plane shown in figure 19. If the line density were dependent on v_{ns} alone, the data would fall on lines inclined at 45° to the axes. The deviations from this behaviour are clearly evident. The irregularity shown probably marks the TI–II transition which somehow must begin in this quadrant, but whose origin is

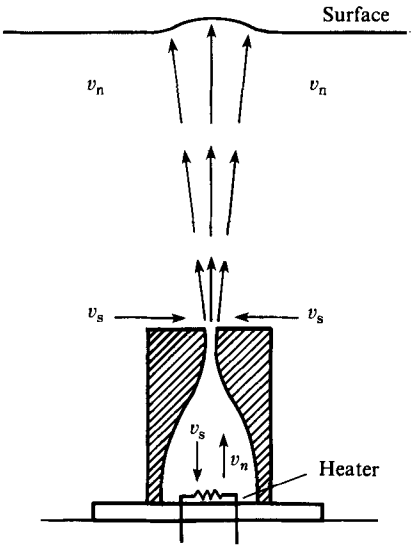

FIGURE 20. The counterflow jet shown in the standard picture in which the superfluid flows into the orifice toward the heater in potential flow and the normal fluid exits as a classical viscous jet which is shown impinging upon a free surface (Liepmann & Laguna 1984).

obscure at present. One important conclusion is that dissipation depends separately on v_n and v_s and not simply on the combination v_{ns}. These elegant data will serve as a basis for future theoretical discussion of these more general flows.

8.2. *The normal jet*

We have described in §2.3 above the pioneering experiments of Kapitza on the jet emerging from a counterflow channel. This interesting flow was ignored for over thirty years until taken up by Liepmann's group at Cal-Tech. A recent review by Liepmann & Laguna (1984) traces much of this modern investigation. The conventional understanding of the jet is shown in figure 20, where the normal fluid exits in a well-defined jet and the superfluid flows back into the orifice in potential flow. This picture leads to the conclusion that the counterflow velocity in the main part of the jet $\boldsymbol{v}_{ns} \approx \boldsymbol{v}_n$. High values of v_{ns} will lead to the formation of vortices in the submerged jet, and therefore vortices should be detectable by thermometry or by second sound.

Dimotakis & Broadwell (1973) carried out an experiment to measure the temperature profile of the jet by traversing a small carbon thermometer along the axis of the jet. The (approximately $\frac{1}{4}$ mm) tube shape was designed in such a way as to have the highest counterflow velocity near the orifice as shown in figure 20. The results showed that the temperature gradient extends only over the region confined by the channel walls near the exit.

In another experiment Laguna (1975) measured the attenuation of second sound in the jet. The jet passed through a plane parallel resonator for second sound, and the change in Q of the resonance was measured. The attenuation in the jet was found to be 15 times less than that expected in a thermal counterflow channel and varied as $q^{\frac{3}{2}}$ instead of q^2.

Liepmann & Laguna (1984) suggest that the measurements described above support the idea that the superfluid is entrained with the jet. This means that there must be a superfluid stagnation point at the orifice with superfluid flow into the

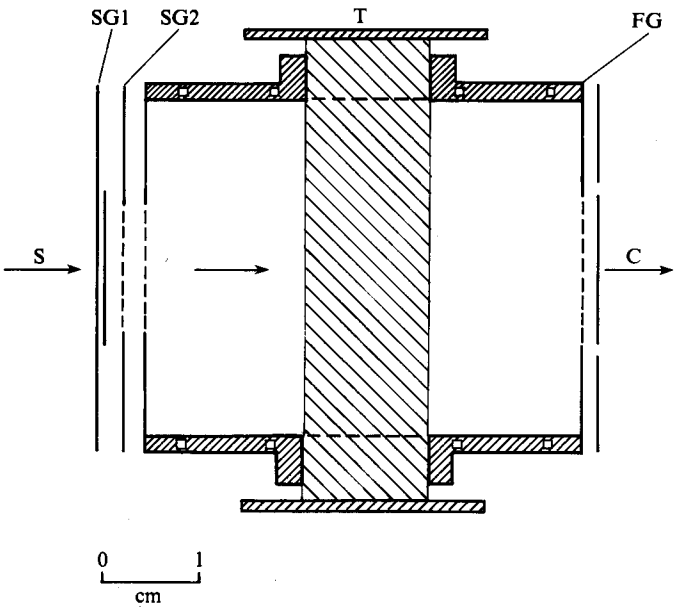

FIGURE 21. Apparatus used by Schwarz & Smith (1981) and Milliken *et al.* (1982) to study ultrasonically generated turbulence. Ions are produced by a radioactive tritium source S and manipulated by screen grids SG1 and SG2 to produce ion pulses. An ion pulse, drifting under the influence of the field determined by SG2 and the Frisch grid FG on the right can be stopped anywhere in the cell by making the drift field zero.

channel and along with the normal fluid jet. Rather than attribute the small attenuation of second sound to vortices in the jet, the authors calculate the scattering of second sound by fluctuations in the jet based on a model by Liepman (1952) for the diffusion of a light ray passing through a turbulent boundary layer. They find non-trivial agreement with helium experiments and theory, and conclude that the superfluid must move with the normal fluid: using v_{ns} in place of v_n gives the wrong temperature dependence. They also conclude that the normal jet is turbulent.

8.3. *Ultrasonically generated turbulence*

A novel form of quantum turbulence generation has been devised by Smith and his colleagues (Carey, Rooney & Smith 1978). Recent experiments (Schwarz & Smith 1981; Milliken, Schwarz & Smith 1982) have utilized the apparatus shown in figure 21. The pair of ultrasonic transducers T set up a strong acoustic field in the cross-hatched region.

The authors believe that the turbulence, which is studied by negative ion trapping, is generated and maintained by acoustic streaming and hence reflects some very complicated physics. The sound has a wavelength of about 10^{-2} cm, hence the experimental regions shown cross-hatched in figure 21, lies in the extreme Fresnel diffraction limit, and the level of acoustic excitation is expected to drop off sharply at the edges of the ultrasonic beam.

The grids SG1 and SG2 (see figure 21) are manipulated to introduce a narrow ion pulse into the main drift space, and it is detected when it reaches the collector C. The attenuation of the pulse caused by ion trapping is a measure of the vortex line density L. The authors, however, introduced a novel technique in which they stopped the pulse (by making the drift field zero) at some point x_0 on the path, and allowed

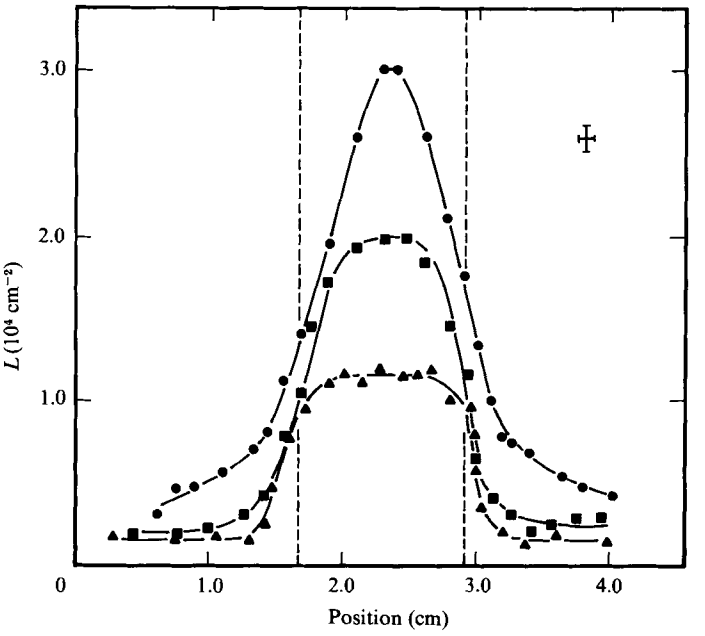

FIGURE 22. Data of Schwarz & Smith (1981) showing the line length per unit volume $L(x_0)$ for various positions x_0 in the drift cell of figure 21. The ultrasound reference level was a few mW/cm^2 and the three curves represent power densities 1 dB (circles), 3 dB (squares), and 5 dB (triangles) below the reference level. The dashed lines show the location of the boundaries of the ultrasonic beam producing the turbulence. The temperature was 1.47 K.

the ions to interact with the local vortex field for an additional time τ_{off}. The drift field is then switched on again, and the remaining free ion pulses are detected at C. Measurement of the attenuation as a function of τ_{off} and at different locations x allowed a direct measure of the spatial structure of turbulent field. Careful experiments were performed to assure that the capture process in the tangle was the same as for capture by uniform vortex lines in a rotating bucket. This information was used to extract the line density $L(x_0)$ from the data.

The data obtained on $L(x_0)$ are shown in figure 22. It appears from the 5 dB curve (triangles) that the turbulence is created more or less homogeneously in the ultrasonic beam. Some line density leaks out and fills the cell at a very low level, the amount leaking out becoming relatively more pronounced as L increases, the profile becoming more peaked and developing pronounced wings.

In a further development with the same apparatus, Milliken *et al.* (1982) examined the decay of the turbulence when the transducers are turned off. Data on the decay taken at the centre of the cell are shown in figure 23. The line in figure 23 comes from an argument about the decay of the tangle which gives an equation essentially the same as that proposed by Vinen (1957*c*), but with a different interpretation.

8.4. *Injected turbulence*

About 1960, H. A. Snyder was investigating second sound absorption in a rectangular rotating resonator made of a porous fired material called Lavite. He discovered that the interior of the resonator, intended to be quiescent for studies of the vortex array in rotation, was filling with turbulence, presumably from turbulence generated in the bath by stirring of the rectangular resonator. Foreman & Snyder (1979) followed up

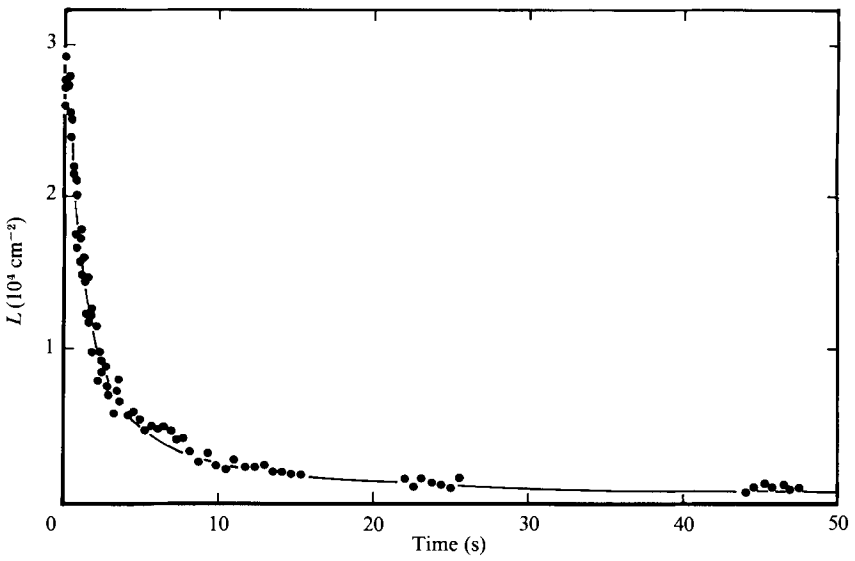

FIGURE 23. Measurements of the free decay of vortex line density L at the centre of the cell taken by Milliken *et al.* (1982).

this unpublished discovery with the apparatus shown in figure 24. Second sound is excited in the upper and lower resonant cavities by Joule heating of a thin silver film applied to a cavity wall. Both cavities are radial mode oscillators and detection is provided by monitoring the change in resistance of Aquadag carbon film applied to the cavity wall. The filters are fine-pore, high-porosity, cellulose-ester filter elements used commonly in biological experiments.

Data were taken by exciting second sound in the lower resonant cavity which passed through a lower filter of 300 nm pore size. Attenuation of second sound was measured in the upper cavity and found to reflect the rotation of the paddle through a 100 nm filter. The attenuation increased with paddle speed and increased with temperature for a given paddle speed. In a further experiment with the upper filter 5000 nm pore size the lower 75 nm pore size, it was shown that the smaller pore size completely blocked the passage of quantized turbulence. Why this apparent size dependence should occur is not known.

d'Humieres & Libchaber (1978) have also studied the self-diffusion of superfluid turbulence through a porous medium, arranged to allow no net mass transport of fluid. The motor-driven propeller creates turbulence which is studied in a resonator equipped for second sound (figure 25). The injection hole was 2 mm in diameter. The authors report that they can transmit vortex rings through media in which the pore size is of diameter larger than the vortex rings.

Several unpublished experiments have been done at Oregon to explore injected turbulence using a counterflow source in place of the propeller of the previous studies. A short counterflow channel with side exits is adjacent to a long closed chamber separated by filter paper. When the counterflow source is operating above a critical heat flux, vorticity fills the isolated chamber and appears to be spatially homogeneous. The magnitude and temperature dependence of the vorticity in the chamber appears to follow the magnitude of vorticity generated by the source in the open channel. The injected turbulence would appear in some sense to be an independent

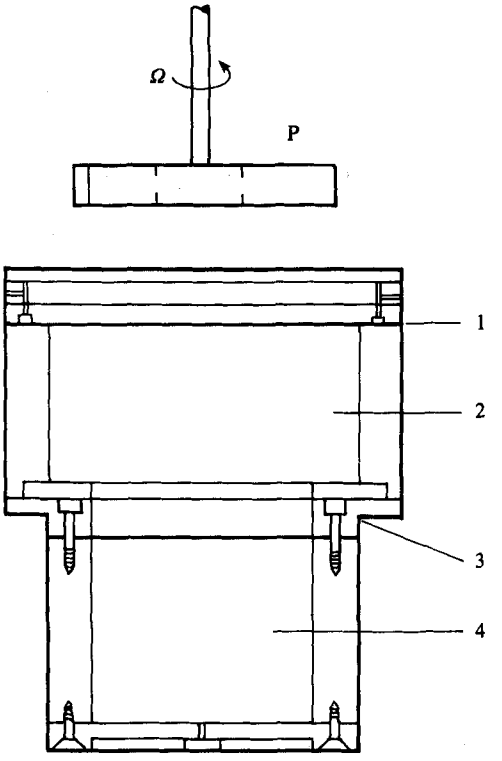

FIGURE 24. Apparatus of Foreman & Snyder (1979) used to study the motion of turbulence through porous filters. The entire apparatus shown is enclosed in a copper shielding can. P, rotating paddle to produce turbulence 1, upper filter; 2, upper cylindrical resonator; 3, lower filter; 4, lower cylindrical resonator.

fluid capable of existing in the long channel in the absence of any mean counterflow. This interesting system appears to deserve more attention.

8.5. *Shock waves*

Second sound shock waves have been studied since Osborne (1951) first reported nonlinear effects in the propagation of second sound. A second-order theory developed by Khalatnikov (1965) and more recently extended by Turner (1979) describes weak shocks. A series of important second sound shock wave experiments have been carried out at Cal-Tech. In 1978, Cummings, Schmidt & Wagner observed a shock-limiting process, which was studied in detail by Turner (1979, 1983). Since shocks produce large counterflow velocities away from the influence of boundaries, it was at first thought that the shock was probing a bulk, or intrinsic, critical velocity in helium II (Turner 1979, 1983). Torczynski (1984*a*, *b*) has shown instead that the shock is limited in its formation, and that this formation is accompanied by the production of large amounts of vorticity. By producing a convergent spherical shock, Torczynski (1984*a*) has produced counterflow velocities as large as 10 m/s, but the shock-limiting processes still occur in the shock formation and not in the bulk.

Although second sound shocks do not yet probe a bulk critical velocity, they do interact in interesting ways with vortex lines, and this interaction depends upon the relative orientation of the propagation direction and the vortex line (Torczynwki

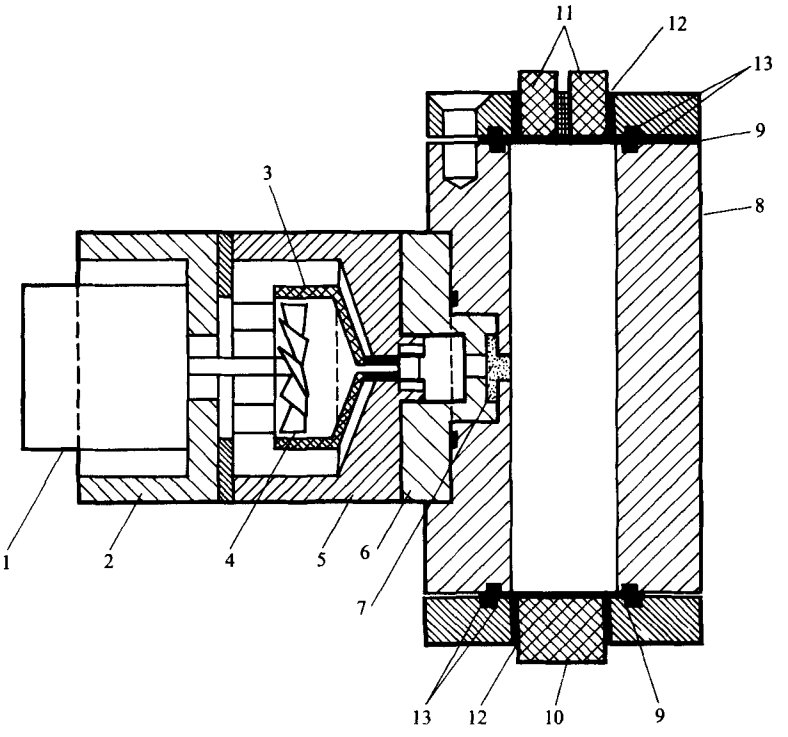

FIGURE 25. Experimental apparatus used by d'Humieres & Libchaber (1978). 1, motor; 2, motor support; 3, funnel; 4, propeller; 5, support of second sound transmitter and receiver; 6, support for porous medium; 7, porous medium; 8, cylindrical cavity; 9, aquadag layer on nuclepore foil 10, fixed electrode for emitter; 11, fixed electrodes for twin detectors; 12, stycast seal; 13, indium O-rings.

1984*b*). This interaction is not yet understood, but could form a useful probe of quantum turbulence.

Some preliminary experiments on shock waves were done using one of the early Oregon channels and reported by Barenghi (1982). Barenghi's experiments, done by attenuation of second sound, allowed him to conclude that vortex lines can be created by shock waves and that the velocity at which the initiation of vorticity is propagated is the velocity of second sound.

9. Open questions and outlook

We hope that the preceding sections have given some indication of why the subject of quantum turbulence interests us, and the sorts of investigations which have been and are being carried out. We now discuss what we believe is to be some of the open questions in this subject, and what the outlook is for progress on them in the near future.

9.1. *Theoretical questions*

Theoretical questions naturally break up into two major divisions: those problems having to do with individual vortex lines, and those having to do with the vortex tangle as a whole.

An example of the former is the microscopic theory of vortex dynamics. This subject, largely the achievement of Vinen and Hall, rests on a series of very careful, often very difficult arguments (see, for example, the recent review by Barenghi *et al.* (1983), which presents two novel arguments for the existence of the Iordanskii force). The difficulty arises because there is no true microscopic theory for helium II, and present models of the core are subject to approximations and guesses. One of the problems plaguing any attempt to invent such a theory is the enormous range of the variables involved. At low temperatures, for example, the collision of a roton with a vortex line is a problem in kinetic theory. Near T_λ, the density of elementary excitations is so large that it is not clear which excitations belong to a vortex line and which are free to interact (Barenghi, Donnelly & Vinen 1985).

The reconnection problem seems to be a fundamental problem in quantum mechanics. There is, however, no known wave function for liquid helium. Quantum calculations generally use the Ginzberg–Pitaevskii equation which is unlikely to be exact, but has a long record of providing reasonable insights. Similarly, the interaction of vortices with boundaries is a relatively new area of study and the problem is far from understood in detail (e.g. Glaberson & Donnelly 1986).

The second class of problems has to do with the behaviour of vortex lines in the bulk. The generalization of forces on a single vortex filament to forces on an array of vortices has always rested on the idea that there is no essential difference, on average, between the two situations. Another assumption sometimes made is that forces on vortices do not react back on the flow that establishes them. The Gorter–Mellink equations (2.4), (2.5) and (2.11) suggest that a high density of vortex lines, at least, will modify the normal fluid velocity field. The modification of Poiseuille flow to nearly uniform flow of the normal fluid at heat fluxes not greatly exceeding critical (figure 10) needs to be understood in some detail.

We have observed in §8.1 that the addition of mass flux to a counterflow produces some qualitative changes, including the disappearance of the TI–TII transition. There are few guesses at present, as to the origin of these effects.

The magnitude and temperature dependence of critical velocities is a problem of long standing in the study of helium II. Theories divide into those concerned with the nucleation of the first vortices in the flow, and those concerned with the growth of pre-existing vorticity. The nucleation problem subdivides further into theories of homogeneous nucleation in the bulk fluid and theories where the presence of boundaries plays an important role in the process. For example, one cannot yet understand the origin of vortices even in equilibrium rotation experiments. A similar lack of understanding exists concerning the magnitude and temperature dependence of the coefficient γ connecting the flow velocities and line densities.

The results on the polarization of the vortex tangle by rotation discussed in §5.9 lead one to ask whether it is possible to say anything meaningful about the statistical mechanics of quantum turbulence. Experience with classical turbulence does not encourage one to be too optimistic, but the quantum turbulence problem offers some simplifying features (§3.3).

9.2. *Experimental questions*

The comparison of classical and quantum turbulence of §3.3 points out the question of the lack of a local probe for quantum turbulence. Indeed, the vortex simulation offers the only insight available today to our problem on a scale comparable to the mean vortex spacing. While no one has yet made a serious attempt to produce a local

probe, it is an open question as to whether the effort to do so would be offset by insight greater than one can achieve by numerical simulation.

One benefit of a local probe would be to try to observe correlations of velocity or vorticity at different times and places in the flow. There have been attempts to observe correlations between (average) fluctuations of vortex line density in different parts of a counterflow, but no notable results have yet emerged.

There have been only a few attempts to push the temperature range in vortex line turbulence experiments beyond the usual 1.2 K–2 K range. But experiments below 1 K, where thermal excitations are nearly absent, and experiments near the lambda transition offers frontiers which have scarcely been examined experimentally. Addition of small amounts of ^{3}He may also afford a new system for investigation.

An underlying question in quantum turbulence is the core structure. Experiments to probe this structure may be possible near T_λ, where the core size diverges.

Induced fluctuations have proved to be relatively easy to understand (§5.7). Intrinsic fluctuations, which might be expected to shed light on the dynamics of the tangle, have been less illuminating than once had been hoped. Not the least of the problems is the realization that bulk motion of the tangle as a whole past a local point of observation will itself produce fluctuations. An associated problem is that we do not know whether the normal fluid is turbulent, and in view of vortex fluctuations, just what that means. If the normal fluid is turbulent, the its own fluctuations are likely to interact with those from the vortices.

Injected turbulence is essentially a completely new area of research. Since vortex line turbulence is associated with motions of v_n and of v_s, the question is how vortex line is produced and maintained in a nearly closed cavity. Are there substantial bulk flows through the filters? Do leaks play a role? If injected turbulence really represents a turbulent vortex line sample in the absence of any mean flow of v_n or v_s, then it is indeed a new and unique form of turbulent flow.

More is known about rotating quantum turbulence (§5.9). This is clearly a very rich system, encompassing a wide range of phenomena ranging from rotation with small heat flow to highly turbulent flow with small rotation. The combination of rotation with more general flows, such as pure superflow, has not yet been attempted.

There are specific questions about steady pipe flow that remain unanswered. For example, the TI–TII transition occurs for small-aspect-ratio channels in counterflow, but not in larger-aspect-ratio channels or in pure superflow. One would like to know how this transition disappears with aspect ratio and with various trajectories in the (v_n, v_s)-plane. Another example is the change in critical velocity with aspect ratio predicted for pure superflow by the simulations, but not yet seen experimentally.

9.3. *Simulation questions*

The most obvious open questions for numerical simulations are the discrepancies with experiment discussed in §7.2. Simulations of a state other than TIV could prove very enlightening.

There are many areas of quantum turbulence research in which simulations have not yet been attempted. Interesting frontiers include turbulence near T_λ, where α' cannot be ignored and where the core structure may become important, transient states (e.g. free decay or turbulence fronts as seen by Peshkov & Tkachenko 1961), and turbulenc with rotation. Injected turbulence would also be an interesting problem for simulations, although it seems that experimental questions may need to be answered first (e.g. what is the applied flow field?).

An unresolved problem is the flattening of the profile of v_n above critical (see §5.5).

Is this due to line–boundary interactions or to normal fluid coupling to the line motion, or both? Does the normal fluid become turbulent? If so, does this force a change in the one-dimensional character of the simulations?

One should also formulate questions for simulations that a local probe might be used to answer. Questions of this nature include correlations of velocity fluctuations, geometric details (e.g. the ratio of interline spacing to radius of curvature, average of higher derivatives of the configuration, etc.), and fluctuations of line density in some given volume.

9.4. *Outlook*

We hope that this paper demonstrates that quantum turbulence is a field with a substantial body of knowledge and substantial current activity, but that has exciting and fundamental questions still to be answered.

We believe that progress in answering these questions will probably require efforts in experiment, theory, and numerical simulations. If it proves possible to account for the principal experimental results by simulations, and if theoretical progress is along the lines generally accepted today, we believe that we shall be in a position before long to say that quantum turbulence is on its way to being understood. By 'understood' we mean that the results of an experiment not yet performed could be predicted by calculations and/or simulations using only the fundamental laws of vortex dynamics.

The authors are very grateful to A. Leonard, P. H. Roberts, K. W. Schwarz, J. T. Tough, C. W. Van Atta, W. F. Vinen and W. T. Wagner for numerous suggestions for improvement of this paper. Our research is supported by the Low Temperature Physics Program of the National Science Foundation under grant DMR 83-13487.

REFERENCES

Ahlers, G. 1969 Mutual friction in HeII near the lambda transition. *Phys. Rev. Lett.* **22**, 54–56.

Allen, J. F. & Misener, A. D. 1938 Flow of liquid helium II. *Nature* **141**, 75.

Anderson, P. W. 1966 Considerations on the flow of superfluid helium. *Rev. Mod. Phys.* **38**, 298–310.

Arms, R. J. & Hama, F. R. 1965 Localized-induction concept on a curved vortex and motion of an elliptical vortex ring. *Phys. Fluids* **8**, 553–559.

Ashton, R. A. & Northby, J. A. 1975 Vortex velocity in turbulent HeII counterflow. *Phys. Rev. Lett.* **35**, 1714–1717.

Awschalom, D. D., Milliken, F. P. & Schwarz, K. W. 1984 Properties of superfluid turbulence in a large channel. *Phys. Rev. Lett.* **53**, 1372–1375.

Baehr, M. L. & Tough, J. T. 1985 Dissipation in combined normal and superfluid flows of HeII: A unified description. *Phys. Rev.* B**32**, 5632-5638.

Baehr, M. L., Opatowsky, L. B. & Tough, J. T. 1983 The transition from dissipationless superflow to homogeneous superfluid turbulence. *Phys. Rev. Lett.* **51**, 2295–2297.

Badash, L. 1985 *Kapitza, Rutherford and the Kremlin.* Yale University Press.

Barenghi, C. F. 1982 Experiments on quantum turbulence. PhD thesis, University of Oregon.

Barenghi, C. F., Donnelly, R. J. & Vinen, W. F. 1983 Friction on quantized vortices in helium II: a review. *J. Low Temp. Phys.* **52**, 189–247.

Barenghi, C. F., Donnelly, R. J. & Vinen, W. F. 1985 Thermal excitation of waves on quantized vortices. *Phys. Fluids* **28**, 498–504.

Barenghi, C. F., Park, K. & Donnelly, R. J. 1981 Absolute measurement of vortex line density in counterflowing HeII. *Phys. Lett.* **84**A, 435–438.

Barenghi, C. F., Swanson, C. E. & Donnelly, R. J. 1982 Induced vorticity fluctuations in counterflowing HeII. *Phys. Rev. Lett.* **48**, 1187–1189.

BAYM, G. & CHANDLER, C. 1983 Hydrodynamics of rotating superfluids 1. *J. Low Temp. Phys.* **50**, 57–87.

BON MARDION, C., CLAUDET, G. & SEYFERT, P. 1978 Steady state heat transport in superfluid helium at 1 bar. In *Proc. 7th Intl. Cryogenic Conf.* pp. 214–221. IPC Science and Technology Press.

BREWER, D. F. & EDWARDS, D. O. 1961 Heat conduction in liquid helium II in capillary tubes I Transition to supercritical conduction. *Phil. Mag.* **6**, 775–790.

CAREY, R. F., ROONEY, J. A. & SMITH, C. W. 1978 Ultrasonically generated quantized vorticity in HeII. *Phys. Lett.* **65**A, 311–313.

CHASE, C. E., 1962 Thermal conduction in liquid helium II: I. Temperature dependence. *Phys. Rev.* **127**, 361–370.

CHASE, C. E., 1963 Thermal conduction in liquid helium II: II. Effects of channel geometry. *Phys. Rev.* **131**, 1898–1903.

CHENG, D. K., CROMAR, M. W., & DONNELLY, R. J. 1973 Influence of an axial heat current on negative ion trapping in rotating He II. *Phys. Rev. Lett.* **31**, 433–436.

CROMAR, M. W. 1977 Turbulence in helium II counterflow in wide channels. PhD thesis, University of Oregon.

CUMMINGS, J. C. 1974 Development of a high performance cryogenic shock tube. *J. Fluid Mech.* **66**, 177–187.

CUMMINGS, J. C., SCHMIDT, D. W. & WAGNER, W. J. 1978 Experiments on second sound shock waves in superfluid helium. *Phys. Fluids* **21**, 713–717.

D'HUMIERES, D. D. & LIBCHABER, A. 1978 Self diffusion of superfluid turbulence through porous media. *J. Physique* C6 **39**, 156–157. See also Hulin, J. P., d'Humieres, D. D., Perrin, B. & Libchaber, A. 1974 Critical velocities for superfluid helium flow through a small hole. *Phys. Rev.* A**9**, 885–892.

DIMOTAKIS, P. E., & BROADWELL, J. E. 1973 Local temperature measurements in supercritical counterflow in liquid helium II. *Phys. Fluids* **16**, 1787–1795.

DONNELLY, R. J. & FRANCIS, A. W. 1985 *Cryogenic Science and Technology Contributions of Leo I. Dana*, Union Carbide Corporation, Danbury.

DONNELLY, R. J. & LAMAR, M. M. 1986 Flow of liquid helium between concentric cylinders: a review. (in preparation).

DONNELLY, R. J. & ROBERTS, P. H. 1969 Stochastic theory of the interaction of ions and quantized vortices in helium II. *Proc. R. Soc. Lond.* A**312**, 519–551.

FEYNMAN, R. P. 1955 Applications of quantum mechanics to liquid helium. In *Progress in Low Temperature Physics*, vol. I (ed. C. J. Gorter), pp. 17–53. North Holland.

FOREMAN, L. R. & SNYDER, H. A. 1979 The penetration of superfluid turbulence through porous filters. *J. Low Temp. Phys.* **34**, 529–538.

GIORDANO, N. 1984*a* Vibrating superleak second-sound transducers. Theory and experiment. *J. Low Temp. Phys.* **55**, 495–526.

GIORDANO, N. 1984*b* Observations of critical velocity effects in vibrating superleak second sound transducers. In *Proc. 17th Intl Conf. on Low Temperature Physics, LR-17*, vol. 1, pp. 307–308. North Holland.

GIORDANO, N. & MUSIKAR, P. 1984 Theory of critical velocity effects in vibrating superleak second sound transducers. In *Proc. 17th Intl Conf. on Low Temperature Physics, LT-17*, vol. 1, pp. 309–310. North Holland.

GLABERSON, W. I. & DONNELLY, R. J. 1986 Structure, distributions and dynamics of vortices in helium II. In *Progress in Low Temperature Physics*, vol. 9 (ed. D. F. Brewer), pp. 1–142. North Holland.

GLABERSON, W. I., JOHNSON, W. W. & OSTERMEIER, R. M. 1974 Instability of a vortex array in helium II. *Phys. Rev. Lett.* **33**, 1197–1200.

GORTER, C. J. & MELLINK, J. H. 1949 On the irreversible processes in liquid helium II. *Physica* **15**, 285–304.

HALL, H. E. & VINEN, W. F. 1956*a* The rotation of liquid helium II: I. Experiments on the propagation of second sound in uniformly rotating helium II. *Proc. R. Soc. Lond.* A**238**, 204–214.

HALL, H. E. & VINEN, W. F. 1956*b* The rotation of liquid helium II: II. The theory of mutual friction in uniformly rotating helium II. *Proc. R. Soc. Lond.* A**238**, 215–234.

HOCH, H., BUSSE, L. & MOSS, F. 1975 Noise from vortex line turbulence in HeII. *Phys. Rev. Lett.* **34**, 384–387.

JONES, C. A. & ROBERTS, P. H. 1982 Motions in a Bose condensate IV Axisymmetric solitary waves. *J. Phys.* A**15**, 2599–2619.

JONES, C. A., PUTTERMAN, S. J. & ROBERTS, P. H. 1986 Motions in a Bose condensate. V. Stability of solitary wave solutions of nonlinear Schrodinger Equations in two and three dimensions. *J. Phys.* A (to appear).

KAPITZA, P. 1938 Viscosity of liquid helium below the lambda point. *Nature* **141**, 74.

KAPITZA, P. 1941 The study of heat transfer in helium II. *J. Phys. USSR* **4**, 181–220.

KEESOM, W. H. & KEESOM, A. P. 1936 On the heat conductivity of liquid helium. *Physica* **3**, 359–360.

KEESOM, W. H., KEESOM, A. P. & SARIS, B. F. 1938 A few measurements on the heat conductivity of liquid helium II. *Physica* **5**, 281–285.

KHALATNIKOV, I. M. 1965 *Introduction to the Theory of Superfluidity*. Benjamin.

LADNER, D. R., CHILDERS, R. K. & TOUGH, J. T. 1976 Helium II thermal counterflow at large heat currents. *Phys. Rev.* B**13**, 2918–2923.

LAGUNA, G. 1975 Second-sound attenuation in a supercritical counterflow jet. *Phys. Rev.* B**12**, 4874–4881.

LIEPMANN, H. W. 1952 Deflection and diffusion of a light ray passing through a boundary layer. *Douglas Rep. S. M.* 14397.

LIEPMANN, H. W., CUMMINGS, J. C. & RUPERT, V. C. 1973 Cryogenic shock tube. *Phys. Fluids* **16**, 332–333.

LIEPMANN, H. W. & LAGUNA, G. A. 1984 Nonlinear interactions in the fluid mechanics of helium II. *Ann. Rev. Fluid Mech.* **16**, 139–177.

LORENSON, C. P., GRISWOLD, D., NAYAK, V. U. & TOUGH, J. T. 1985 Dynamic features of superfluid turbulence near the second critical heat current. *Phys. Rev. Lett.* **55**, 1494–1497.

MANTESE, J., BISCHOFF, G. & MOSS, F. 1977 Vortex line density fluctuations in turbulent superfluid helium. *Phys. Rev. Lett.* **39**, 565–568.

MARTIN, K. P. & TOUGH, J. T. 1983 Evolution of superfluid turbulence in thermal counterflow. *Phys. Rev.* B**27**, 2788–2799.

MILLIKEN, F. P., SCHWARZ, K. W. & SMITH, C. W. 1982 Free decay of superfluid turbulence. *Phys. Rev. Lett.* **48**, 1204–1207.

MURRAY, C. A., WOERNER, R. L. & GREYTAK, T. J. 1975 High resolution study of the two-roton bound state. *J. Phys.* C**8**, L90–L94.

OBERLEY, C. E., & TOUGH, J. T. 1972 Evidence for the hydrodynamic origin of critical heat currents in helium II. *J. Low Temp. Phys.* **7**, 223–228.

ONSAGER, L. 1949 A remark following a paper by Gorter at a conference in Florence. *Nuov. Cim.* **6**, Supp. 2, 249.

OPATOWSKY, L. B. & TOUGH, J. T. 1981 Homogeneity of turbulence in pure superflow. *Phys. Rev* B**24**, 5420–5421.

OSTERMEIER, R. M., CROMAR, M. W., KITTEL, P. & DONNELLY, R. J. 1980 Fluctuations in turbulent He II counterflow. *Phys. Lett.* **77** A, 321–324.

OSBORNE, D. V. 1950 The rotation of liquid helium II. *Proc. Phys. Soc. Lond.* **63**, 909–912.

OSBORNE, D. V. 1951 Second sound in liquid helium II. *Proc. Phys. Soc. Lond.* **64**, 114–123.

PESHKOV, V. P. & TKACHENKO, V. K. 1961 Kinetics of the destruction of superfluidity in helium. Zh. Eksp. Teor. Fiz. **41**, 1421–1432 [*Sov. Phys., J. Exp. Theor. Phys.* **14**, 1019–1022].

PFOTENHAUER, J. M. & DONNELLY, R. J. 1985 Heat transfer in liquid helium. In *Advances in Heat Transfer*, vol. 17 (ed. J. P. Hartnett & T. F. Irvine,), pp. 65–158. Academic.

PFOTENHAUER, J. M., LUCAS, P. G. J. & DONNELLY, R. J. 1984 Stability and heat transfer of rotating cryogens: Part II. Effects of rotation on heat-transfer properties of convection in liquid He^4. *J. Fluid Mech* **145**, 239–252.

ROBERTS, P. H. & DONNELLY, R. J. 1973 Dynamics of rotons. *Phys. Lett.* **43** A, 1–2.

ROBERTS, P. H. & DONNELLY, R. J. 1974 Superfluid mechanics. *Ann. Rev. Fluid Mech.* **6**, 179–225.

ROBERTS, P. H. & PARDEE, W. J. 1974 Bound States of the two-roton Schrodinger equation. *J. Phys.* A 1283–1292.

SCHWARZ, K. W. 1978 Turbulence in superfluid helium: steady homogeneous counterflow. *Phys. Rev.* B **18**, 245–262.

SCHWARZ, K. W. 1982*a* Free decay of superfluid turbulence. *Phys. Rev. Lett.* **48**, 1204–1207.

SCHWARZ, K. W. 1982*b* Generating superfluid turbulence from simple dynamical rules. *Phys Rev. Lett.* **49**, 283–285.

SCHWARZ, K. W. 1983 Critical velocity for a self-sustaining vortex tangle in superfluid helium. *Phys. Rev. Lett.* **50**, 364–367.

SCHWARZ, K. W. 1985 Three-dimensional vortex dynamics in superfluid ^{4}He. I. Line–line and line–boundary interactions. *Phys. Rev.* B **31**, 5782–5804.

SCHWARZ, K. W. & SMITH, C. W. 1981 Pulsed-ion study of ultrasonically generated turbulence in superfluid ^{4}He. *Phys. Lett.* **82** A, 251–254.

SLEGTENHORST, R. P., MAREES, G. & VAN BEELEN, H. 1982 Steady flow of helium II in the presence of a heat current. *Physica* **113** B 341–366; also Slegtenhorst, R. P., Marees, G. & van Beelen, H. 1982 Transient effects in superfluid turbulence. *Physica* **113** B, 367–379.

SMITH, C. W. & TEJWANI, M. J. 1984 Fluctuations of a negative ion current in turbulent He II. *Phys. Lett.* **104** A, 281–284.

SWANSON, C. E. 1985 A study of vortex dynamics in counterflowing helium II. PhD thesis, University of Oregon.

SWANSON, C. E., BARENGHI, C. F. & DONNELLY, R. J. 1983 Rotation of a tangle of quantized vortex lines in He II. *Phys. Rev. Lett.* **50**, 190–193.

SWANSON, C. E. & DONNELLY, R. J. 1985 Vortex dynamics and scaling in turbulent counterflowing helium II. *J. Low Temp. Phys.* **61**, 363–399.

SWANSON, C. E., WAGNER, W. T., BARENGHI, C. F. & DONNELLY, R. J. 1986 Calculation of the frequency and velocity dependence mutual friction parameters in helium II. (in preparation).

TENNEKES, H. & LUMLEY, J. L. 1972 *A First Course in Turbulence.* Massachusetts Institute of Technology Press.

TORCZYNSKI, J. R. 1984*b* Converging second sound shock waves in superfluid helium. *Phys. Fluids* **27**, 1138–1141.

TORCZYNSKI, J. R. 1984*b* On the interaction of second sound shock waves and vorticity in superfluid helium. *Phys. Fluids* **27**, 2636–2644.

TOUGH, J. T. 1982 Superfluid Turbulence. In *Progress in Low Temperature Physics*, vol. 8 (ed. D. F. Brewer), pp. 133–219. North Holland.

TOWNSEND, A. A. 1961 A continuum theory of the isothermal flow of liquid helium II. *J. Fluid Mech.* **10**, 113–132.

TURNER, T. N. 1979 Second sound shock waves and critical velocities in liquid helium II. PhD thesis, California Institute of Technology.

TURNER, T. N. 1983 Using second-sound shock waves to probe the intrinsic critical velocity of liquid helium II. *Phys. Fluids* **26**, 3227–3241.

VINEN, W. F. 1957*a* Mutual friction in a heat current in liquid helium II. I. Experiments on steady heat currents. *Proc. R. Soc. Lond.* A **240**, 114–127.

VINEN, W. F. 1957*b* Mutual friction in a heat current in liquid helium II. Experiments on transient effects. *Proc. R. Soc. Lond.* A **240**, 128–143.

VINEN, W. F. 1957*c* Mutual friction in a heat current in liquid helium II. III. Theory of mutual friction. *Proc. R. Soc. Lond.* A **242**, 493–515.

VINEN, W. F. 1958 Mutual friction in a heat current in liquid helium II. IV. Critical heat currents in wide channels. *Proc. R. Soc. Lond.* A **243**, 400–413.

VINEN W. F. 1966 Vortices in superfluid systems. In *Quantum Fluids* (ed. D. F. Brewer), pp. 74–108. North Holland.

WANG, R. T., SWANSON, C. E. & DONNELLY, R. J. 1986 Anisotropy and drift of a quantum vortex tangle. To appear.

YARMCHUK, E. J. & GLABERSON, W. I. 1979 Counterflow in rotating superfluid helium. *J. Low Temp. Phys.* **36**, 381–429.